

**Matrix Isolation Infrared and *ab-initio* Study of Hydrogen Bonded
Complexes of N-Heterocyclic Carbene and Water**

Sumit Kumar Agrawal

MS12099

A dissertation submitted for the partial fulfillment of

BS-MS dual degree in Science



Indian Institute of Science Education and Research, Mohali

April 2017

Certificate of Examination

This is to certify that the dissertation titled “Matrix Isolation Infrared and *Ab-Initio* Study of Hydrogen Bonded Complexes of N-heterocyclic Carbene and Water ” submitted by Mr. Sumit Kumar Agrawal (Reg. No.: MS12099) for the partial fulfillment of BS-MS dual degree programme of the Institute has been examined by the thesis committee duly appointed by the Institute. The committee finds the work done the candidate satisfactory and recommends that the report be accepted.

Dr. Sugumar Venkataramani

Dr. P. Balanarayan

Dr. Arijit Kumar De

Prof. K.S. Viswanathan

(Supervisor)

Dated: 21st April, 2017

Declaration

The work presented in this dissertation has been carried out by me under the guidance of Prof. K. S. Viswanathan at the Indian Institute of Science Education and Research Mohali. This work has not been submitted in part or in full for degree, a diploma, or a fellowship to any other university or institute. Whenever contributions of others are involved, every effort is made to indicate this clearly, with due acknowledgement of collaborative research and discussions. This thesis is a bonafide record of original work done by me and all source are listed within have been detailed in the bibliography.

Sumit Kumar Agrawal

(Candidate)

Dated:21stApril, 2017

In my capacity as the supervisor of the candidate's project work, I certify that the above statements by the candidate are true to the best of my knowledge.

Prof. K. S. Viswanathan

(Supervisor)

Acknowledgement

I would like to express my special thanks to my Supervisor Prof. K.S. Viswanathan who gave me the golden opportunity to do this wonderful project on the topic “Matrix Isolation Infrared and *Ab-Initio* Study of Hydrogen Bonded Complexes of N-Heterocyclic Carbene and Water”, for sharing his pearls of wisdom with me during the course of this project, which also helped me in doing a lot of Research and I came to know about so many new things . His dedication and keen interest above all his overwhelming attitude to help his students had been solely and mainly responsible for completing my work. His timely advice, meticulous scrutiny and scientific approach have helped me to great extent to accomplish this MS final year project.

I am also thankful to my Master’s thesis committee members Dr. P. Balanarayan, Dr. Sugumar Venkataramani and Dr. Arijit Kumar De for their valuable comments and suggestions during the committee meeting.

I am also immensely grateful to Dr. Sanjay Singh, Deependra, Prashanth for providing me the NHC and the use of their laboratory instruments and the wonderful discussions. I am extremely thankful to Prof. N. Sathyamurthy, Director of IISER Mohali, for allowing me to use the various facilities of this institute to carry out research work.

I am also very thankful to other lab members, Bhupendra, Mamta, Sandeep, Sudha for help in carbene handling and NMR analysis.

My special thanks to Ginny Karir for helping and motivational support during entire project.

I am extremely thankful to my other lab members Kanupriya, Jyoti, Pankaj, Ravi, Sruthy and Dr. Anamika for the useful discussions during the research. I would also like to thank each of my friends and classmates who were always there for me for the entire 5 years course.

I also thank my family for supporting me at every stage of life. I would like to thank the Department of Science and Technology (DST), India for providing INSPIRE fellowship.

List of figures

Figure	Figure Caption	Page no.
Figure 1	Representation of nature of frontier orbital of divalent carbon	1
Figure 2	Orbital Structure of Singlet and Triplet Carbene	2
Figure 3	Reactivity of Singlet and Triplet Carbene	2
Figure 4	Molecular diagram of carbene showing inductive effect of substituents	3
Figure 5	Molecular diagram of carbene showing mesomeric effect of substituents	4
Figure 6	Energy difference between singlet and triplet carbene	4
Figure 7	Preparation of the stable 1,3-di-1-adamantylimidazolin-2-ylidene (IAd) as the first representation of free carbene	5
Figure 8	A schematic representation of hydrogen bond formation	6
Figure 9	Structure of NHC-H ₂ O complex and NHC-MeOH complex	8
Figure 10	(a) structure of 1,3-di-isopropyl-4,5-dimethylimidazol-2-ylidene (b) water	9
Figure 11	A schematic representation of isolation of sample and deposition	10
Figure 12	A Schematic representation of parts of matrix isolation setup	13
Figure 13	(a) Photograph of Cryostat and (b) Block Diagram of Cryostat	14
Figure 14	(a) Internal parts of second stage expander (b) A schematic Diagram of cryostat parts containing optical extension set	15
Figure 15	a) Experimental setup b) Experiment in process	17
Figure 16	¹³ C NMR of 1,3-diisopropyl-4,5-dimethylimidazol-2-ylidene	21

	before the experiments	
Figure 17	^{13}C NMR of 1,3-diisopropyl-4,5-dimethylimidazol-2-ylidene	
	after the experiments	22
Figure 18	^1H NMR Spectra of 1,3-diisopropyl-4,5-dimethylimidazol-2-ylidene	22
Figure 19	Spectra of Nujol, Carbene in Nujol and computed spectra of carbene	23
Figure 20	Computed IR spectra of Carbene, Water and Complex	
	at MP2/6-311++G(d,p)level of theory	26
Figure 21	Structures of optimized geometries obtained for the	
	five deferent complexes	27
Figure 22	Spectral feature of 1,3-diisopropyl-4,5-dimethylimidazol-2-ylidene	29
	in N_2 matrix (a) after annealing (b) before annealing	
Figure 23	Experimental spectra of H_2O in N_2 Matrix in the ratio of (5:1000) at 12K	30
Figure 24	Experimental spectra of D_2O in N_2 matrix in the ratio of (5:1000) at 12K	30
Figure 25	Comparison of IR spectra of complex, NHC and H_2O .	31
	(A) before annealing (B) After the Annealing.	
	(a) $\text{NHC}(7^0\text{C}):\text{H}_2\text{O}:\text{N}_2(5:1000)$, (b) $\text{NHC}(7^0\text{C}):\text{N}_2(1000)$ and	
	(c) $\text{H}_2\text{O}:\text{N}_2(5:1000)$	
Figure 26	Comparison of IR spectra of complex, NHC and D_2O .	32
	(A) before annealing (B) After the Annealing.	
	(a) $\text{NHC}(7^0\text{C}):\text{D}_2\text{O}:\text{N}_2(5:1000)$, (b) $\text{NHC}(7^0\text{C}):\text{N}_2(1000)$ (c) $\text{D}_2\text{O}:\text{N}_2(5:1000)$	
Figure 27	AIM structures of all complexes	34

List of tables

Table	Table Heading	Page no.
Table 1	Table of typical chemical shift in C^{13} NMR spectrum	21
Table 2	Relationship between dihedral angle of all conformer	24
Table 3	Computed stabilization energy (in Kcal/mol) of NHC- H_2O Raw/ZPE/BSSE corrected energy values	28
Table 4	Aim calculations for 1,3-diisopropyl-4,5-dimethylimidazol-2-ylidene and water complexes	35
Table 5	Some selected geometrical parameters of complexes at M062X/6-311++G(d,p) and MP2/6-311++G(d,p), where bond length is given in Å, bond angle in degree	36

List of Abbreviations

NHC	N-Heterocyclic Carbene
BSSE	Basis set superposition error
ZPE	Zero point energy
AIM	Atoms-in-molecules
FCC	Face centered cubic
FTIR	Fourier Transform Infrared

CONTENTS

	Page No.
List of Figures	v
List of Tables	vii
List of Abbreviations	viii
Abstract	xi
Chapter 1: Introduction	1-9
1.1 Carbenes	1
1.1.1 Carbenes Structure and Spin Multiplicity	1
1.1.2 N-Heterocyclic Carbenes	5
1.2 Spectroscopic methods of studying carbenes	5
1.3 The Hydrogen Bond	6
1.4 Current research in hydrogen bonding complexes of carbenes	7
1.5 Motivation for the present work	8
Chapter 2: Matrix Isolation Technique and Experimental Setup	10-19
2.1 Matrix Isolation Technique	10
2.2 Advantages of matrix isolation spectroscopy	11
2.3 Matrix environmental effect	11
2.4 Instrumentation setup	13
2.4.1 Matrix isolation infrared setup	13
2.4.2 FTIR spectrometer	16
2.5 Experimental procedure	16
2.6 Computational procedure	1

2.6.1	Geometry optimization	18
2.6.2	Basis set superposition error (BSSE)	18
2.6.3	AIM analysis	19
Chapter 3:	Result and Discussion	20-39
3.1	Isolation and characterization of NHC	
3.1.1	NMR study	20
3.1.2	FTIR study	21
3.2	Computational results	24
3.2.1	Conformational analysis:	24
3.2.2	Calculation for possible complexes	25
3.2.3	Optimized geometries obtained at MO62x/6-311++G(d,p) and MP2/6-311++G(d,p) for complexes of NHC with Water	26
3.3	Experimental	28
3.3.1	Matrix isolation infrared spectra of NHC	28
3.3.2	Matrix isolation IR of H ₂ O and D ₂ O	29
3.3.3	Matrix isolation IR of NHC-H ₂ O and NHC-D ₂ O complexes	31
3.3.4	Experimental and vibrational analysis	32
3.4	AIM analysis	33
3.5	Discussion	38
Chapter 4:	Conclusions	39

Bibliography

Abstract

Carbenes are neutral species having six electron in valance shell. Their incomplete octet and coordinative unsaturation, it makes unstable and they have only traditionally studied as highly reactive species. But after the emergence of N-Heterocyclic Carbenes (NHC's) in 1991 it opened a new class of research in organic chemistry and in transition metal chemistry, with numerous applications. Many experimental techniques is available to study carbenes. Matrix isolation infrared spectroscopy in one such technique in which carbenes can be trapped at very low temperature and provide long life time to study. This technique has advantage of small line width, which is efficient to study weak bonded complexes like hydrogen bond and various conformations.

Very recently, hydrogen bonding interaction studied between carbene and proton donor solvent as $R_2C \cdots H-X$. The nucleophilic nature of NHC provides strong hydrogen bonding site with the proton donor solvents like H_2O , $MeOH$.

I am currently working on the conformational analysis and the weak interaction study of the "N-heterocyclic carbene" using Matrix Isolation FTIR Spectroscopy supported by *ab-initio* calculations. In this work, the hydrogen bonded complexes of N-heterocyclic carbene with water have been studied. The main aim of this work is to investigate the structure of the various hydrogen bonded complexes between the precursor molecules. The computational work has been performed at **R-B3LYP**, **M06-2X** and **MP2** level of theories using 6-311++G (d,p) basis set. The interaction between N-heterocyclic carbene carbon and hydrogen of proton donor solvent ($NHC \cdots H-OH$) has been observed as a dominating interaction in the optimized ground state. To study these complexes experimentally, the matrix isolation experimental facility has been used.

INTRODUCTON

1.1 Carbenes

1.1.1 Carbene Structure and Spin Multiplicity

Carbenes are neutral species, in which the carbene carbon has two nonbonding electrons, which may be in a singlet or triplet state. The carbene carbon is also covalently bonded to other atoms. In classical carbene systems, the carbene is attached covalently to two other carbons, such as dimethyl or diphenyl carbene. It is also possible that the carbene carbon may be attached to hetero atoms, such as N, S, O. The class of carbenes where hetero atom involved is nitrogen has become one of the popular systems in recent times – the N-heterocyclic carbene, which also happens to be theme of study of this work.

Singlet carbenes result from a σ^2 or $p\pi^2$ configuration while the triplet carbene from a $\sigma^1p\pi^1$ configuration.

The geometry of the carbene can be linear, described by sp -hybridization of the carbene carbon and two nonbonding electrons occupy p_x and p_y orbitals, where p_x and p_y are two degenerate orbitals. In the bent geometry, the carbene carbon adopts an sp^2 -hybridization and two non-bonding electrons occupy p_x and p_y orbitals which are non-degenerateⁱ. Due to bending p_y orbital remain unchanged and is denoted as $p\pi$, whereas p_x orbital acquire some s -character and is denoted as σ which leads to stabilization as shown in fig.1. The orbital structure of singlet and triplet carbene as shown in fig.2ⁱⁱ.

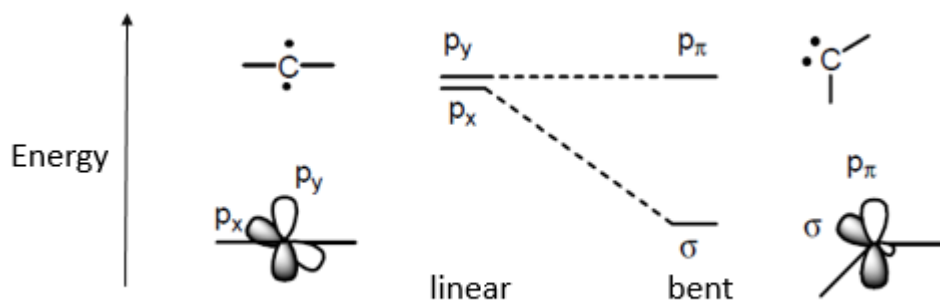


Figure 1: Representation of nature of frontier orbital of divalent carbonⁱⁱ

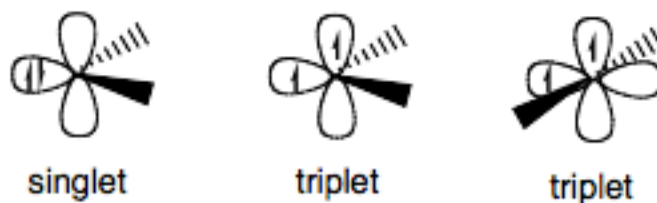


Figure 2: Orbital Structure of Singlet and Triplet Carbene

Reactivity of carbenes

The multiplicity of carbene carbon atom decides primarily the reactivity of carbenesⁱⁱⁱ. Singlet and triplet carbenes behave differently as the former generally acts as an electrophile participating in pericyclic reactions or can also act as nucleophiles. Triplet carbenes are known to be biradicals and they show step wise addition reactions^{iv} (Fig. 3).

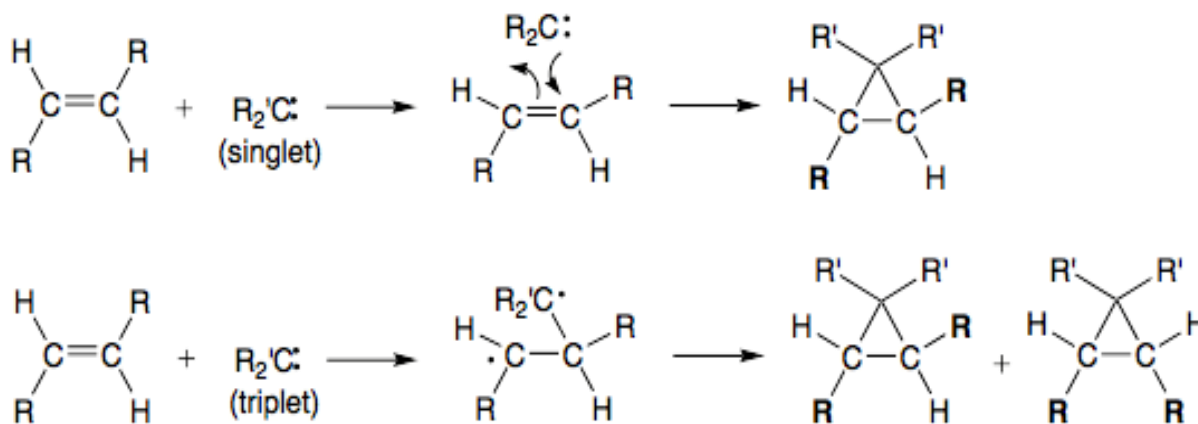


Figure 3: Reactivity of Singlet and Triplet Carbene

Stability of carbenes

The substitutes on the carbene carbon, through the operation of the inductive and mesomeric effects, mainly decide the stability of the carbenes. Steric effects may also play a role.

Inductive effect: Electron- withdrawing substituents (Cl, O, N) attached to the carbene atom render stability to the singlet. σ -electron-withdrawing substituents induce more s-character in p_x orbital, resulting in a lowering the energy of σ orbital. Therefore the energy gap σ - $p\pi$ increase and favors the singlet state^v. On other hand if σ -electron-donating substituents are attached to

the carbene atom, they induce less of an s-character in p_x orbital, resulting in small σ - p_π gap^v, thus favoring the triplet state as shown in **fig. 4**.

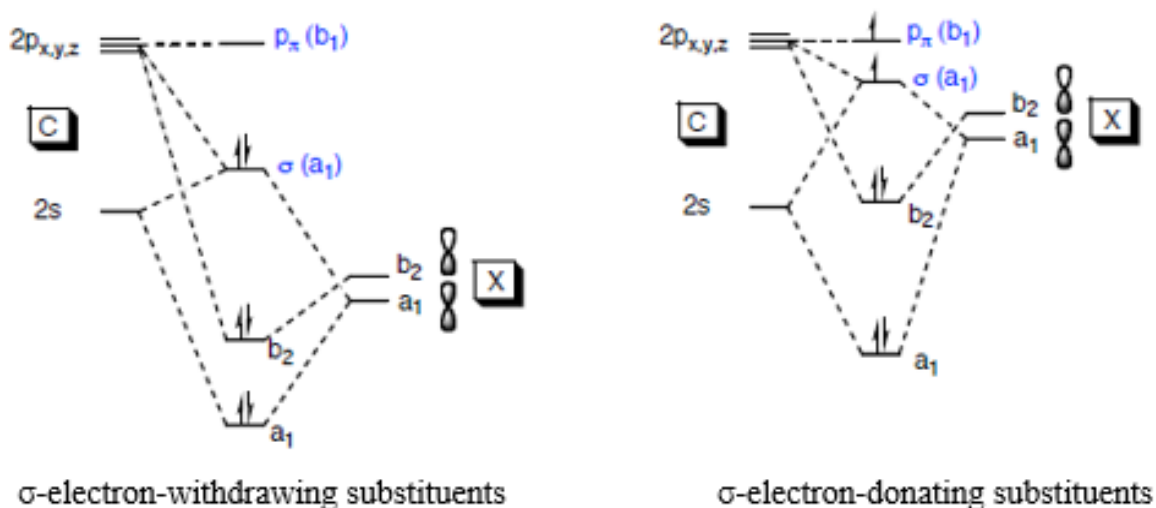


Figure 4: Molecular diagram of carbene showing inductive effect of substituents

Mesomeric effect: Mesomeric effect can be understood in terms of interaction of the carbon orbital (σ , p_π or p_x , p_y) and the p or π orbital of the carbene substituents. If there are π -electron-donating substituents (X) such as $-F$, Cl , Br , NR_2 , PR_2 , $O-R$, these can interact with the vacant p orbital, increasing the energy of p orbital. The σ orbital remain unchanged and the σ - p_π gap increases which favors the singlet bent state. Whereas π -electron-withdrawing group(Y) such as $-COR$, CN , SiR , BR_2 imparts a linear singlet state. If both types of substituents(X & Y) are attached then quasi-linear carbene^{vi} is formed as shown in **fig.5**.

Usually carbenes are very reactive; however, some carbenes, the singlet carbenes, are thermodynamically stable in the absence of moisture and can be isolated and stored. The triplet carbenes on the other hand have half-life of a few seconds. These species can only be observed in experiments, but cannot be stored.

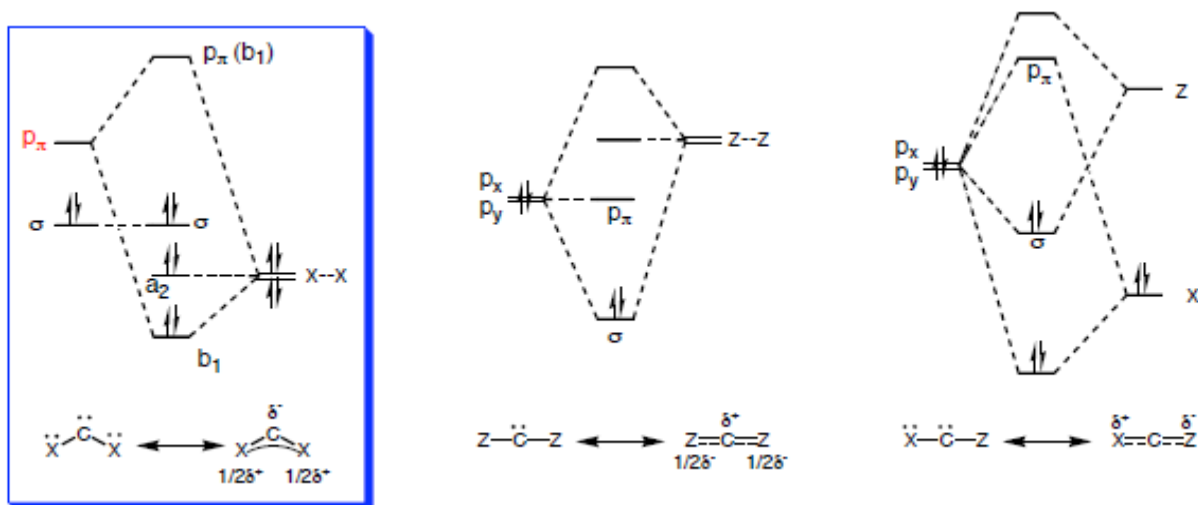


Figure 5: Molecular diagram of carbene showing mesomeric effect of substituents

Energy of singlet and triplet carbenes

In general triplet carbenes are more stable than singlet; the triplet being therefore the ground state. However, substituents can influence the state of the carbene. If there are electron donating groups that can donate electron pair into empty p-orbital of carbene, this may stabilize the singlet state by delocalizing the pair of electrons. If energy of the singlet state is sufficiently reduced, it can then actually become the ground state.

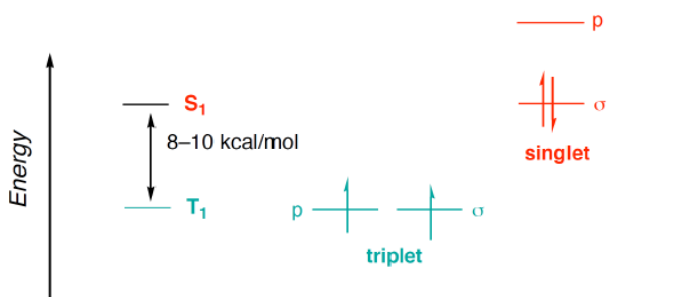


Figure 6: Energy difference between singlet and triplet carbene^{iv}

The positive sign of $\Delta E_{st} = E_{\text{singlet}} - E_{\text{triplet}}$ means that the ground state is triplet.

1.1.2. N-Heterocyclic carbenes

With the emergence of N-heterocyclic carbenes^{vii}, a new direction has been launched in the study of carbene chemistry. NHC's are generally singlet carbenes in which divalent carbon atom is attached to at least one nitrogen atom. In early 1960's Wanzlick first investigated the existence of NHC^{viii}. NHC's are electron rich species and can serve as good σ donor ligands. They can form strong complexes with metals^{vii}.

The first free stable carbene was prepared by in 1991 Arduengo and co-workers by using a strong base sodium hydride (NaH) and the catalytic amount of dimethylsulfoxide (DMSO) in tetrahydrofuran (THF)^{ix} as shown in **fig.7**. The use of polar aprotic solvent DMSO facilitates dissolution of N-heterocyclic carbene precursor salt for a homogenous reaction without interfering with the de-protonation process and gives normal carbene^{ix}.

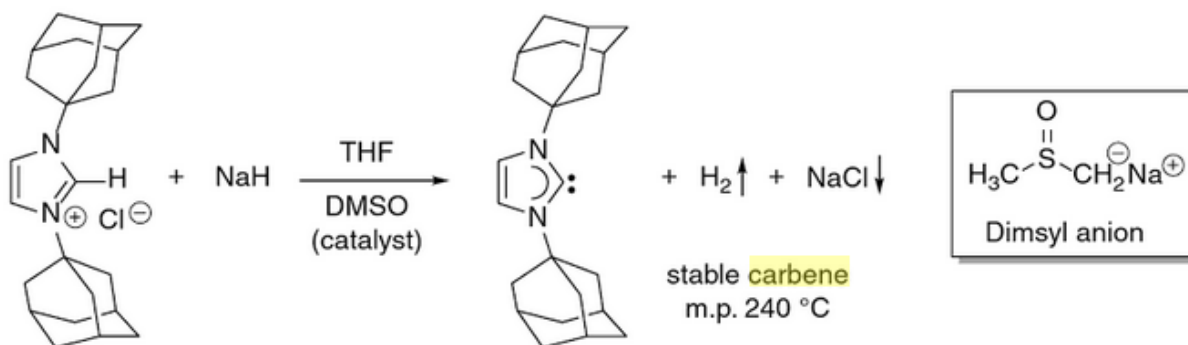


Figure 7: Preparation of the stable 1,3-di-1-adamantylimidazol-2-ylidene (IAd) as the first representation of free carbene

1.2. Spectroscopic methods of studying carbenes

One of the most widely used techniques for investigation of carbene is Matrix Isolation Infrared Spectroscopy. The technique of matrix isolation is used to trap the reactive species which are then probed using spectroscopic techniques such as IR, UV/Vis and ESR. Where IR spectroscopy is used as the probe, N₂ or Ar, which are transparent in the infrared region, are used as the matrix gases. Hydrocarbon glasses, popularly referred to as Schpolskii matrices, are used in UV/Vis or ESR studies.^x

As will be shown later, matrix IR spectroscopy in combination with computations serves as a power tool in the study of the structure and binding of carbenes.

In this work, we have attempted to study the hydrogen bonding interactions of NHC with water, which can be expected to involve a strong hydrogen bond. We will now therefore discuss the nature and importance of the hydrogen bond.

1.3 The hydrogen bond

Hydrogen bond is a non-covalent interaction between two polar groups that occurs when hydrogen comes between two more electronegative atoms like F, O, N etc^{xi}. Hydrogen bond can be denoted as X-H...Y, where X is the donor atom and Y is the acceptor atom. Depending upon the geometry of the molecule and environment of the molecule the energy of hydrogen bond lie between 1-40kal/mol. Hydrogen bond is stronger than van der Waals forces and weaker than ionic and covalent bond. Hydrogen bonding interactions is well known to influence a large number of processes in chemistry, biology, physics and material science. The stability of the DNA and protein structures are some of the celebrated examples of the importance of the hydrogen bond. Molecular conformations in chemistry and reaction pathways have been guided by these interactions. A few of the hydrogen bonded structures are shown in **fig 8**.

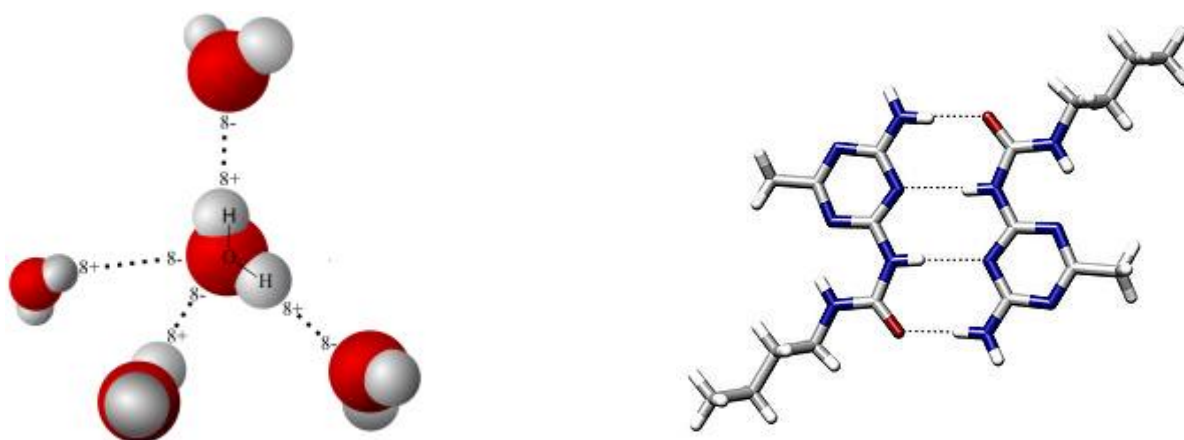


Figure 8: A schematic representation of hydrogen bond formation

Hydrogen bond studies

Matrix isolation infrared spectroscopy is a powerful technique to study hydrogen bond interactions. The formation of X-H...Y bond results in the weakening of the covalent X-H bond, which leads to a decrease of X-H frequency. This is called red shift in X-H stretch in which electron is transferred from the proton acceptor to an anti-bonding orbital of X-H which causes a weakening of X-H bond and a consequent shift to lower frequency. Some atypical examples have been observed where there is a shift to higher frequency region of X-H bond, which are popularly known as blue shifted hydrogen bonds^{xii,xiii}.

Computational chemistry is used to investigate the hydrogen bond and for a corroboration with experiments^{xiv}. In this work we used **R-B3LYP**, **M06-2X** and **MP2** methods using 6-311++G(d,p) basis set to investigate the hydrogen bonded interaction, between 1,3-di-isopropyl-4,5-dimethylimidazol-2-ylidene and H₂O.

1.4 Current research in hydrogen bonding complex of carbene:

Very recently, Raut *et al.* investigated the hydrogen bonded complexes of 1,3-dimethylimidazol-2-ylidene with H₂O and MeOH^{xv}. The hydrogen bonded complexes of NHC-H₂O and NHC-MeOH were found to be significantly stronger than many typical hydrogen bonded complexes. This conclusion was arrived at from the observed large red shifts in frequency of H₂O and MeOH (583cm⁻¹ & 546cm⁻¹ respectively) as a result of complex formation.

The experimental results were also supported by *ab-initio* calculation at MP2 and M062x methods using 6-311++G(d,p) and aug-cc-pVDZ basis set. The interaction energy of NHC with H₂O and MeOH was computed to be 9.1kcal/mol and 9.8kcal/mol respectively, which indicates strong basic character of NHC's.

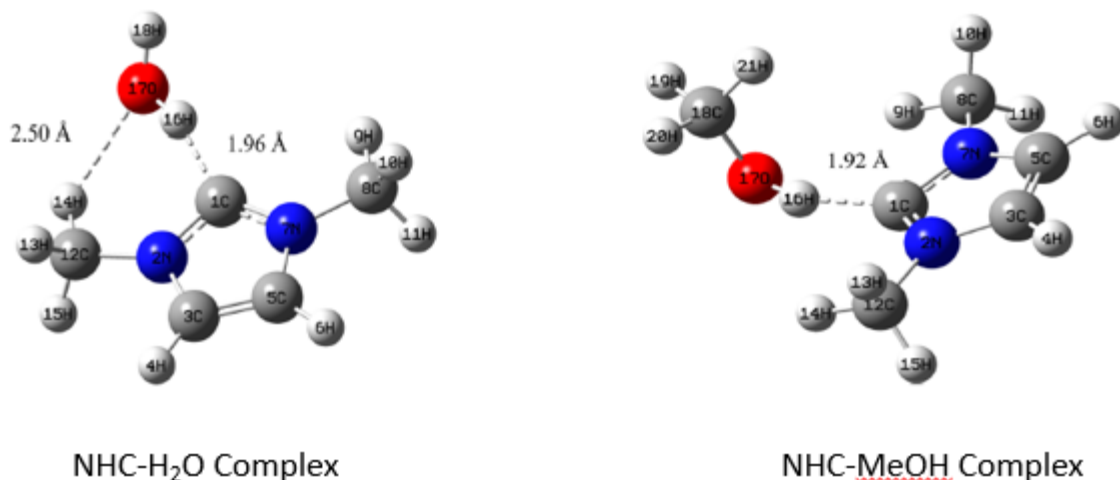


Figure 9: Structure of NHC-H₂O complex and NHC-MeOH complex

Recently Sander and Costa also investigated hydrogen bonded complex of diphenylcarbene and MeOH using EPR and infrared spectroscopy^{xvi}. They found very strong hydrogen bond giving rise to 864cm^{-1} frequency shift in O-H stretch. Interestingly they also found that the spin state of the NHC is changed from triplet to singlet state as a result of the hydrogen bond formation.

1.5 Motivation for the present work

It has been a challenge to study NHC and their complexes. Matrix isolation is ideally suited for this purpose. NHC's are very reactive species and are capable of displaying very strong hydrogen bonding owing to the presence of highly nucleophilic carbene carbon. Literature reports presents only one experimental study of the hydrogen bonded complexes of NHC till date. Raut *et al.* used 1,3-dimethylimidazol-2-ylidene (NHC) which was generated *in situ* from the carboxylate precursor. This NHC was found to form hydrogen bonded complexes with an interaction energy of 9 kcal/mol with H₂O and MeOH in the matrix. This method of NHC generation was accompanied by formation of huge amounts of CO₂ as a byproduct of precursor pyrolysis in the matrix which pose a difficulty in complete and clean spectral analysis of NHC hydrogen bonded complexes. In order to resolve this difficulty, we used 1,3-diisopropyl-4,5-dimethylimidazol-2-ylidene (NHC) which is a stable carbene. This carbene could be directly deposited in the matrix without any accompanying by-products produced during the deposition process. This NHC is however moisture sensitive and very reactive, and one therefore had to

exercise great caution in sample preparation and deposition. In the present study complexes of 1,3-diisopropyl-4,5-dimethylimidazol-2-ylidene (NHC) with H₂O and D₂O were co-deposited and studied for complex formation. The experiments were corroborated with computational studies. To aid in the understanding of the possible structures of the NHC-water complex, we show below the potential active sites of NHC and water to indicate hydrogen bond sites:

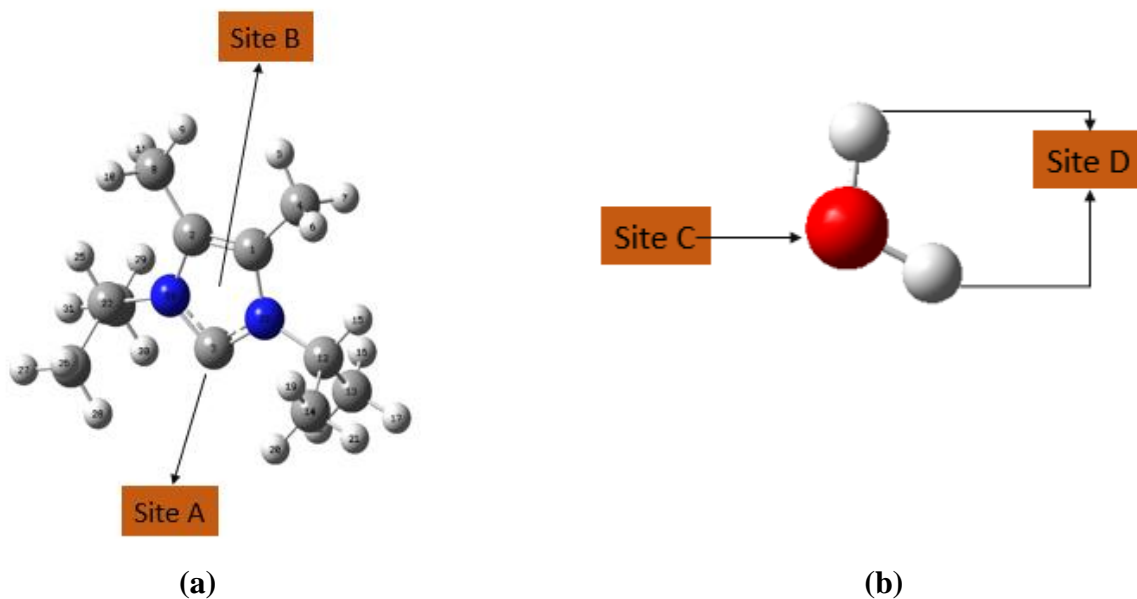


Figure 10: (a) Structure of 1,3-di-isopropyl-4,5-dimethylimidazol-2-ylidene and (b) Water

In 1,3-di-isopropyl-4,5-dimethylimidazol-2-ylidene, both nucleophilic carbene carbon and π -cloud (Site A & Site B respectively) act as proton acceptor and the hydrogens of H₂O (Site D) acts as proton donor. The oxygen of H₂O (Site C) also acts as proton acceptor.

This multiple site of precursor molecules leads to several hydrogen bonded complexes and our aim is to investigate the all possible complexes than can be formed. Matrix isolation infrared spectroscopy provides us to investigate all local minima as well as global minimum.

Chapter 2

Matrix Isolation Technique and Experimental Setup

This section deals with experimental setup of matrix isolation infrared spectroscopy, which is used to study hydrogen bonded complex of N-heterocyclic carbene with H₂O and D₂O. This section also deals with the instrumentation parts of matrix isolation technique and experimental setup that is used to study the complexes of NHC-H₂O and NHC-D₂O.

2.1 Matrix isolation technique

Matrix isolation is a technique in which guest molecules are trapped in the rigid host materials at very low temperature (12K). Host material for this technique that are generally used are inert gases like N₂, Ar, Ne and Xe. This technique was first developed by George C. Pimentel in mid-1950, to study free radicals^{xvii}. This technique is a very powerful for the studies on unstable and reactive species like carbene, nitrenes etc. In this technique the typical guest:host sample ratio is 1:1000 or 1:100000 which ensures 99% isolation. Because the guest molecules are embedded in a host material, the diffusion process and bimolecular reactions cannot take place. The sample and the inert gas are deposited on to the KBr or CsI window and studied by infrared spectroscopy. Quartz window is used for studied UV-Vis Spectroscopy. Electron spin resonance spectroscopy also studied where the deposition is done on sapphire-tipped copper rods.

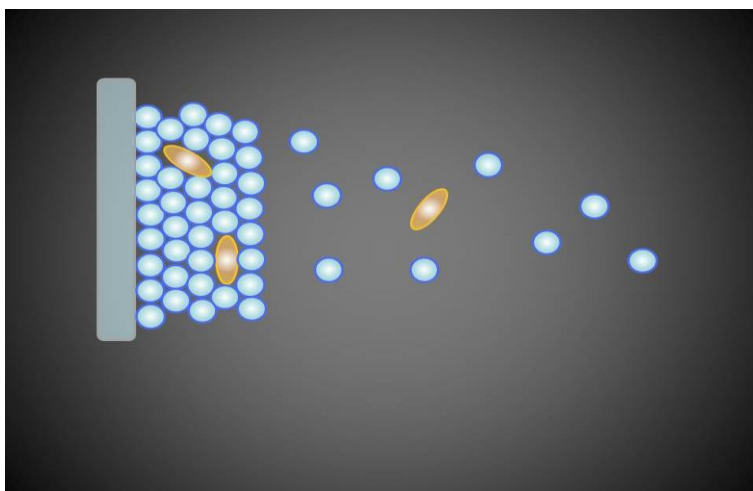


Figure 11: A schematic representation of isolation of sample and deposition

2.2 Advantage of matrix isolation technique

The inert gases used in this technique which do not react with the guest molecules. Inert gases are mostly monoatomic except N₂, all of which do not infrared absorptions and are therefore ideally suited for vibrational spectroscopy.

In the inert gas cage, the molecules do not experience any intermolecular interactions because of the isolation in the solid matrix. Doppler and Collisional broadening also absence because molecules are immobilized in frozen matrix. Since molecules are trapped at very low temperature, therefore electronic and vibrational levels of molecules are less populated.

Owing the all reasons, the matrix isolated spectra are sharp and simple unlike condensed phase spectra that have large spectral line widths.

2.3 Matrix Environmental Effects

Even though the matrix in these experiments are inert gases, and are not expected to perturb the chemistry and spectroscopy of the trapped species, they nevertheless perturb the spectra for various reasons. We discuss some of the effects below:

a) Matrix shifts:

The guest molecules are trapped in the inert matrix and still experience very weak interaction with the matrix which result in a shift in the frequency or splitting of bands. The long range London dispersion forces and the short range repulsive forces are two dominant forces for this interaction. This frequency shift, $\Delta\nu$ in a matrix with respect to the gas phase value arises from electrostatic ($\Delta\nu_{\text{elec}}$), including ($\Delta\nu_{\text{ind}}$), dispersive ($\Delta\nu_{\text{dis}}$) and repulsive interaction ($\Delta\nu_{\text{rep}}$) and is given by the following expression^{xviii}

$$\Delta\nu = (\nu_{\text{matrix}} - \nu_{\text{gas}}) = \Delta\nu_{\text{elec}} + \Delta\nu_{\text{ind}} + \Delta\nu_{\text{dis}} + \Delta\nu_{\text{rep}}$$

A theoretical treatment of matrix induced frequency shift has been given by Pimental and Charles. It has been shown that a tight cage usually introduces a blue shift in vibrational frequencies (relative to the gas phase values) and a loose cage a red shift.^{xix}

b) Multiple trapping sites:

The guest species are trapped in the matrix in either substitutional site or interstitial holes. Different trapping sites have different kind of intermolecular interaction with the matrix and trapped species.

Therefore different matrix cage induces different shifts in the band. Splitting of the band can be easily identified by changing the matrix, since different matrix do not have same trapping sites.

c) Aggregation:

In matrix isolation the guest species and matrix ratio in experiment are 1:1000, which conform the 99% isolation. By increasing the concentration of guest species there is chances to form dimer, trimmer. If two guest species are trapped very close to each other, then modification in vibrational band can be observed due to overlap of their respective cages. The probabilities of intermolecular interaction to ensure the maximum isolation of analyte molecules can be calculated by formula $P = (1-r)^{12}$, where r is the reciprocal of the matrix ratio. For very small value of r the expression becomes $P = (1-12r)$, from this it is clear that the matrix ratio of 1000 is needed to ensure 99% isolation^{xx}.

d) Matrix structure:

All inert gas matrix except helium crystalizes in face centered cubic (FCC)^{xxi}. In FCC crystal, a guest species is trapped in the substitutional site where host molecule is replaced by guest species. Guest species are trapped by 12 nearest matrix atoms. It not possible to guest molecule to accommodate one substitutional site replacing the one host molecule. So generally more than one substitutional sites are occupied by the guest molecule. A site with 18 nearest atoms is created by removing two matrix atoms.

In addition to substitutional site, crystal lattice can also have interstitial sites, Tetrahedral sites (T) and octahedral sites (O). A tetrahedral site has 4 nearby matrix atoms, whereas octahedral site has 6 nearby matrix atoms. A guest molecule with a spherical diameter of 0.159 Å and 0.293 Å can be accommodated in Tetrahedral and octahedral site respectively.

2.4 Instrumentation setup:

The main components of matrix isolation setup involve cryostat, vacuum system and FTIR spectrometer. The photograph of matrix isolation IR spectroscopy of our lab and its main components are shown in the following **figure 12**.

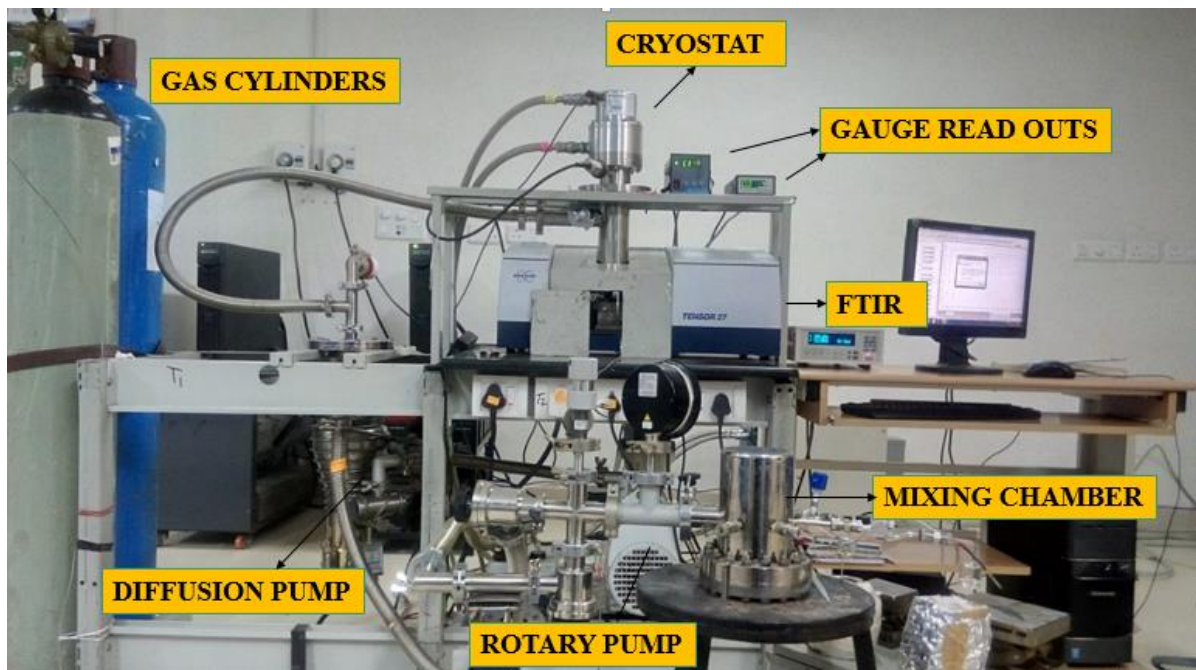


Figure 12: A Schematic representation of parts of matrix isolation setup

2.4.1 Matrix Isolation Infrared Setup

The main parts of matrix isolation setup are:

1. Cryostat
2. Vacuum System

(1) Cryostat:

Cryostat is used to get cryogenic temperature which is required to solidify the inert gas and also helps to form matrix structure. The matrix gases like Ar, Ne, Xe, N₂ are requires a very low temperature of around 10-15K for forming solid matrix. The common cryogenic fluids used in cryostat to obtain low temperature are liquid N₂, liquid He, liquid H₂. Closed cycle cryostats are also available working on the principle of a Gifford-McMahon cycle to generate very low temperature (~77K and 12K) and using He as the working fluid.

In our system helium compressor is used to produce 10K temperature which is equipped with the cryostat CH-202w/HC4E1 model (Sumitomo Heavy industries Ltd.).The helium compressor is cooled with the 3kW chiller unit. (Fig. 13)

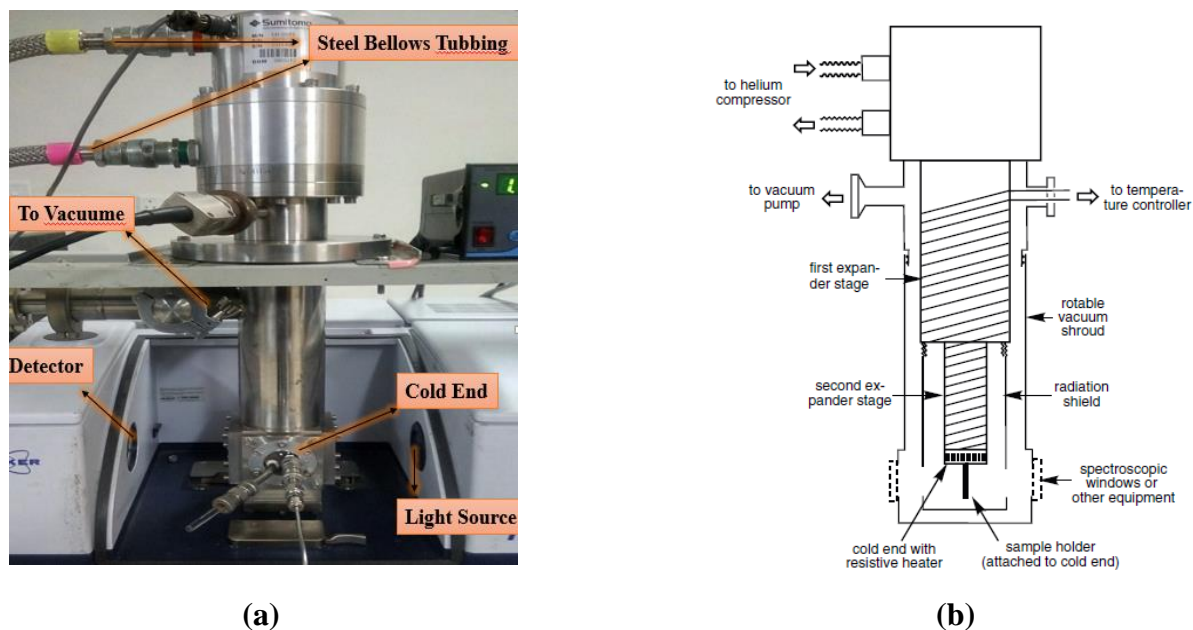


Figure 13: (a) Photograph of Cryostat and (b) Block Diagram of Cryostat

The cryostat can further subdivided into four main components:

- a) Cold head
- b) A helium compressor
- c) Temperature control unit
- d) An optical extension set

Cold head and a helium compressor

The lowest temperature achieved by this cryostat which uses He in GM cycle is around 10K. The cold head is connected to compressor by two stainless steel bellows tubes and electrical power cable. One of the bellows tube supplies high pressure Helium gas from compressor to cold head, other bellows tube returns low pressure Helium gas from cold head. Evacuation of the assembly is done through vacuum port mounted on the on the expander as shown in **fig.13**. The heat generated during the compression of the gas of the compressor and diffusion pump can be removed by chiller.

Temperature control unit

In our cryostat temperature is measured by silicon diode sensor. At the cold end of cryostat there is heater coil which can regulate the temperature 12K to 300K. To anneal the matrix we increase the temperature upto 27K for N₂ matrix and 35K for Ar matrix. Annealing enhances the diffusion and promotes the reaction of trapped species.

An optical extension set

A optical extension set consist a substrate holder, radiation shield and vacuum jacket. A KBr window is mounted on the substrate holder. Sample deposition happens on the KBr window. It is the cold end of the cryostat where the temperature is around 12K. This KBr window surrounded by radiation shield which is made up of copper. The vacuum jacket has four ports. Another vacuum jacket is attached with this vacuum jacket through O ring seal.

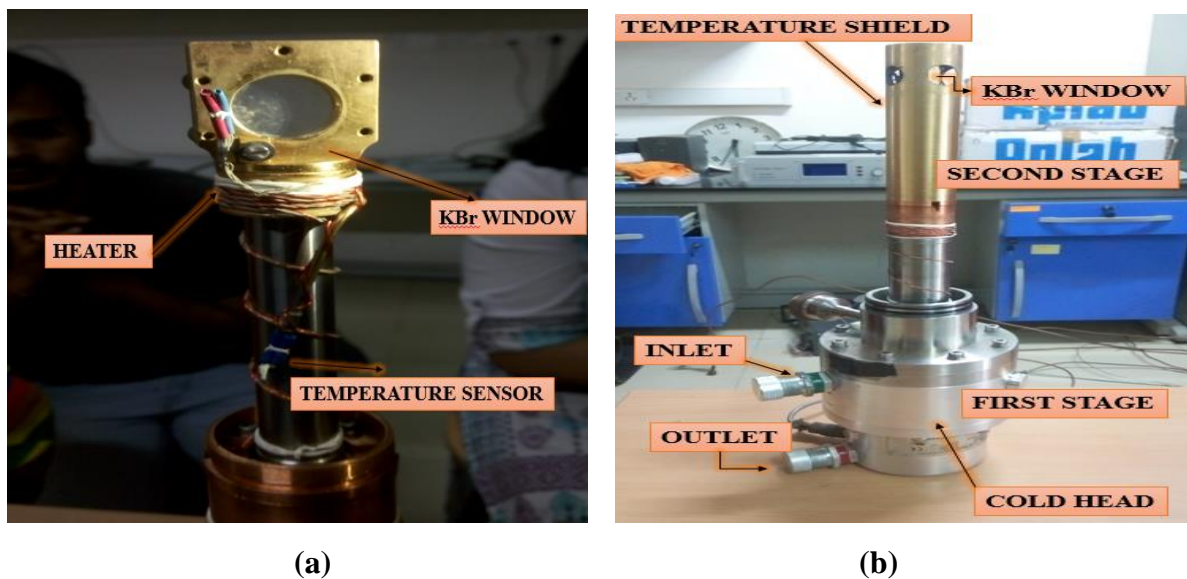


Figure 14: (a) Internal part of second stage expander (b) A schematic diagram of cryostat parts containing optical extension set

(2) Vacuum system

There are two types of pumping system used in this setup.

a) Rotary pump b) Diffusion pump

The rotary pump is basically a mechanical pumps which remove the air from the system by rotary devices. The average vacuum can maintained by this pump around 10^{-3} mbar. These pumps have mainly two purpose:

a) They remove bulk of the air which is initially at atmospheric pressure b) Since diffusion pump cannot exhaust against atmospheric pressure so backing of diffusion pump it used. The pumping speed of rotary pumps are 100 lit/min.

Diffusion pump can produce vacuum up to 10^{-6} mbar. The pumping speed of diffusion pump is ~ 300 lit/min and is backed by a rotary pump. It is made up of stainless steel chamber containing vertically stacked cone-shaped jet assemblies. At the base of chamber there is an oil container in which generally silicon oil used. Oil has very low vapor pressure and it is heated by an electric heater. The vapor of the oil move upward and is expelled through jet assemblies. To cool the chamber, cold water flow around the chamber through the coil outside coil.

2.4.2 FTIR spectrometer

To record an infrared spectrum, we have used Fourier transformed infrared spectroscopy. Broker Tensor 27 FTIR spectrometer was used for our experiments operating at a resolution of 0.50 cm^{-1} for recording the spectrum in the spectral range $4000\text{-}400 \text{ cm}^{-1}$.

2.5 Experimental procedure

The carbene 1,3-diisopropyl-4,5-dimethylimidazol-2-ylidene was weighed (~ 11 mg) inside a glove box and taken into sample holder. The initial pressure of the system was 2.6×10^{-6} mbar. In another glass bulb, H_2O or D_2O was taken. The glass bulb was thoroughly degassed, subjected to several freeze-pump-thaw cycles before deposition, in order to eliminate any trapped gaseous impurities. We have done our experiments using both single jet and double jet nozzles.

In the single jet method, we mixed D₂O (~5mbar) with N₂ in mixing chamber. After preparation of mixing chamber we set-up our carbene sample holder system, to the desired temperature (~7C) to get enough concentration of NHC as shown in figure 15. Once the desired temperature was reached, the deposition of the mixture of matrix gas and water or deuterium oxide was done for 15 minutes. After completion of the deposition, a spectrum was recorded. The KBr substrate was then warmed to 27 K and held at this elevated temperature for 30 minutes and then returned to 12 K. The spectrum of matrix thus annealed was again recorded. After every experiment, the vacuum system was opened and cleaned before the start of the next experiment.

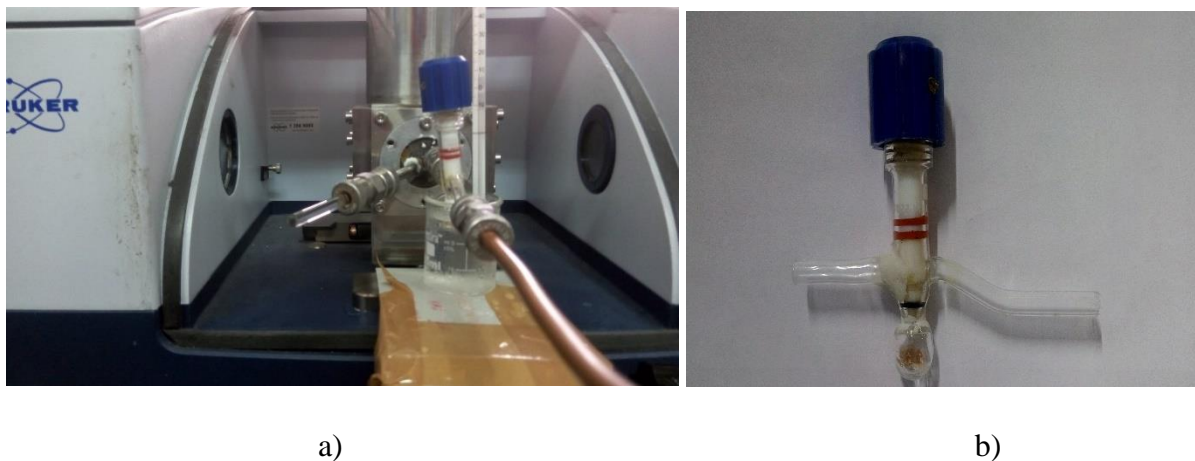


Figure 15: a) Experimental setup b) Sample Holder

2.6 Computational procedure

Hartree-Fock (HF), density functional (DFT) and Møller-Plesset perturbation theory(MP2), Configuration interaction(CI), coupled cluster(CC), Multi-Configurational self-consistent field(MCSCF), etc. are some of the popular electron structure methods used for *ab-initio* calculations^{xxii}.

The computational study was carried out using Gaussian 09^{xxiii} package in Linux operating system. The computational work has been performed at **R-B3LYP**, **MO6-2X** and **MP2** method using 6-311++G (d,p) basis set. To examine the nature of interactions between the monomers of complexes, AIM (Atoms in molecule) package was also used.

2.6.1 Geometry optimization

In computational chemistry geometry optimization is first performed to arrive at the structure of the system, which corresponds to the minimum on the potential. At this point the forces on the atom are zero and is also referred to as a stationary point.^{xxiv}

After optimization we get most stable configuration of the molecule, which may correspond to the local minima or global energy minima. That these are stationary point structures is confirmed by a vibrational frequency calculation, which must ensure that all frequencies are positive.^{xxv}

2.6.2 Basis Set Superposition Error (BSSE)

When the energy of complex (E_{AB}) is computed, the basis function used are those of both the monomer subunits. For computing the energy of individual monomers (E_A and E_B), the basis function pertaining to only corresponding monomers are used. As the number of basis function used is large in the computation of complex, the energy obtained will be lower. In complex, basically each monomer can use the basis functions of other. Stabilization energies thus derived from the calculated energies E_A , E_B and E_{AB} will be overestimated and the error is referred to as the basis set superposition error (BSSE). The best way to estimate BSSE is to increase the basis set until the stabilization energy is stable to desired accuracy. The commonly used method to correct for BSSE is by counterpoise correction proposed by Boys and Bernadi. In this scheme, the energies of monomer E_A and E_B and the complex E_{AB} are calculated in the same basis set spanned by the functions of the complex AB and the difference is obtained as follows:

$$\Delta E = E_{AB}(AB) - [E_A(AB) + E_B(AB)]$$

Where, E_A = Energy of the monomer A using the basis set AB

E_B = Energy of the monomer B using the basis set AB

E_{AB} = Energy of the complex AB using the basis set AB

BSSE corrected term is evaluated as follows:

$$\text{BSSE correction} = \{[E_A(A) - E_B(AB)] + [E_B(B) - E_B(AB)]\}$$

The BSSE correction term turns out to be positive. Which this term is added to the raw stabilization energy, a negative quantity, and overall BSSE corrected energy becomes less negative.

2.6.3 AIM Analysis:

For performing the AIM analysis, we first generated wave functions corresponding to optimized geometry of our complexes using the Gaussian09 package. From the electron density information, we obtain the bond critical points, charge density (ρ) and the Laplacian of charge density ($\Delta^2\rho$). If the first derivative of $\rho(r)$ is zero at point of space r then that point will correspond to a critical point, where the $\rho(r)$ will be minimum, maximum or can be saddle point. The second derivative of $\rho(r)$ at this point gives whether the function will be maximum or minimum. Positive sign corresponds to minimum and negative sign corresponds to maximum at this point. The rank of critical point (ω) which is equivalent to the number of non-zero eigen values or non-zero curvature of ρ at the critical point and the signature (σ) is the algebraic sum of the signs of the eigen values. The critical point is denoted by (ω, σ) . For example (3,-1) critical point means, there is three non-zero curvature and one positive and two negative eigen value. A (3,-1) correspond to the bond between two atoms, a (3,+1) corresponds to the a ring, a (3,+3) corresponds to the a cage.^{xxvi}

The sum of the three Hessians ($\lambda_1, \lambda_2, \lambda_3$) at the critical point, gives the Laplacian of charge density($\Delta^2\rho$) which provides us useful information, in which the electronic charge density is distributed in the inter nuclear region. For the hydrogen bonded complex the charge density at the critical point is around $10^{-2} e/(\text{bohr})^3$ and the Laplacian of the charge density is positive.

Chapter 3

Result and Discussions

In this chapter we will discuss our results on the study of the 1,3-diisopropyl-4,5-dimethylimidazol-2-ylidene (NHC) and its complexes with water as well as deuterium oxide using computation and matrix isolation technique. NHC's have strong nucleophilic character at the carbene carbon and π -cloud of the ring, which provides strong hydrogen bond interaction with water. We will also discuss the isotopic shift in the frequency of water and D₂O. The experimental procedure and computational methods used in this work has already been discussed in chapter 2.

3.1 Isolation and Characterization of NHC

1,3-diisopropyl-4,5 dimethylimidazol-2-ylidene was synthesized using KI in dry THF giving the stable NHC. It was solid, orange brown in color, which was sensitive to air so, which could therefore be handled only in a glove box.

3.1.1 NMR Study:

Before use, the carbene was characterized using NMR. Both ¹H and ¹³C NMR spectra of 1,3-diisopropyl-4,5 dimethylimidazol-2-ylidene were recorded. In particular the feature at 207 ppm in the ¹³C NMR confirmed the product to be the carbene. The assignment of the other carbon atoms in the NHC are given in Table 1. Proton NMR spectra were also recorded that confirm the identity of the substrate that we were using in our experiments. After the experiment, NMR spectra were again recorded of the substrate remaining after the deposition of the matrix, to ensure that the carbene was in fact intact during all of the experiments. The persistence of the 207 ppm feature due to the carbene ensure that the carbene was intact in all the experiments conducted. The NMR spectra are shown in **Fig. 16** and **fig.17**.

Carbon environment	Chemical shift(ppm)
C=C (in alkenes)	115 - 140
RCH ₂ NH ₂	30 - 65
R ₂ CH ₂	16 - 25
RCH ₃	10-15
Carbene carbon	<190

Table 1: Table of typical chemical shift in C¹³ NMR spectra

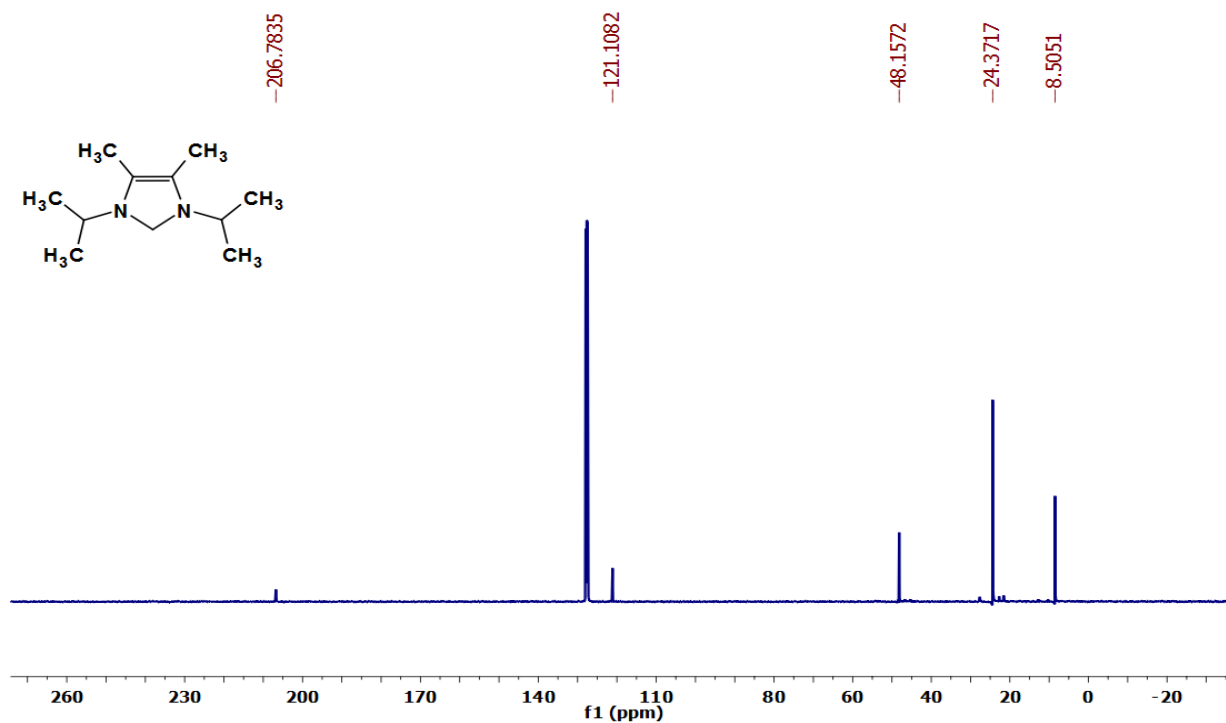


Figure 16: ¹³C NMR of 1,3-diisopropyl-4,5-dimethylimidazol-2-ylidene before the experiments

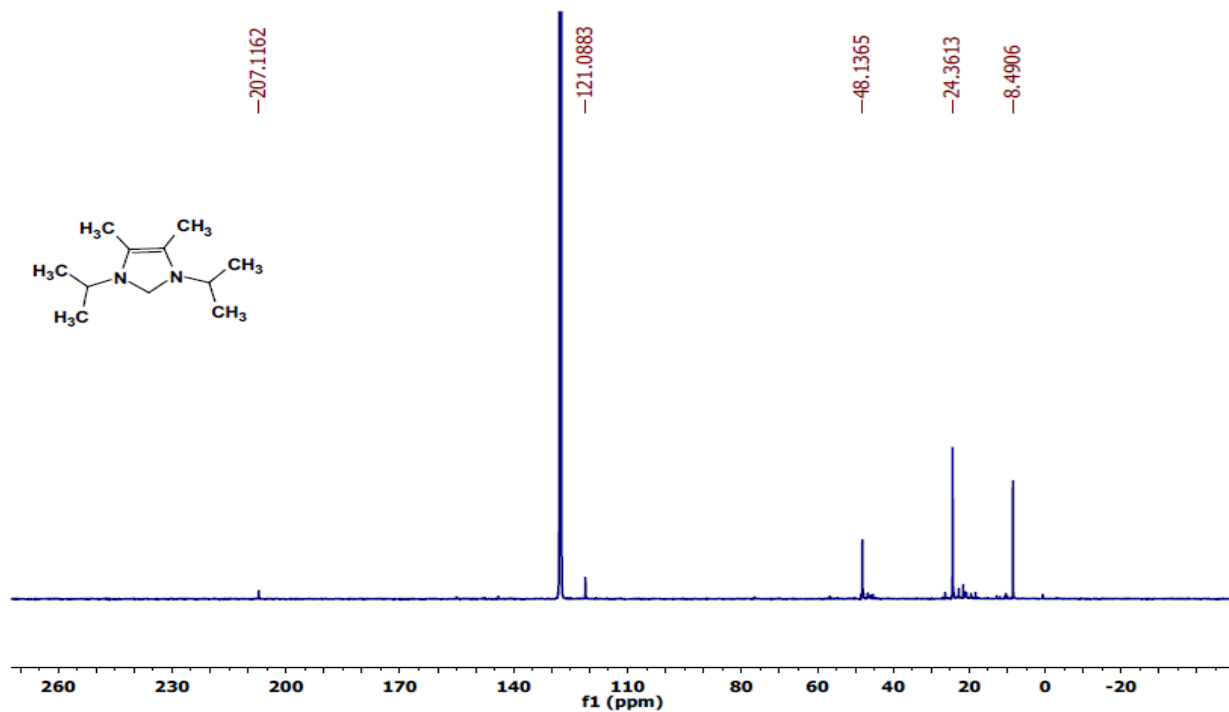


Figure 17: ^{13}C NMR of 1,3-diisopropyl-4,5-dimethylimidazol-2-ylidene before the experiments

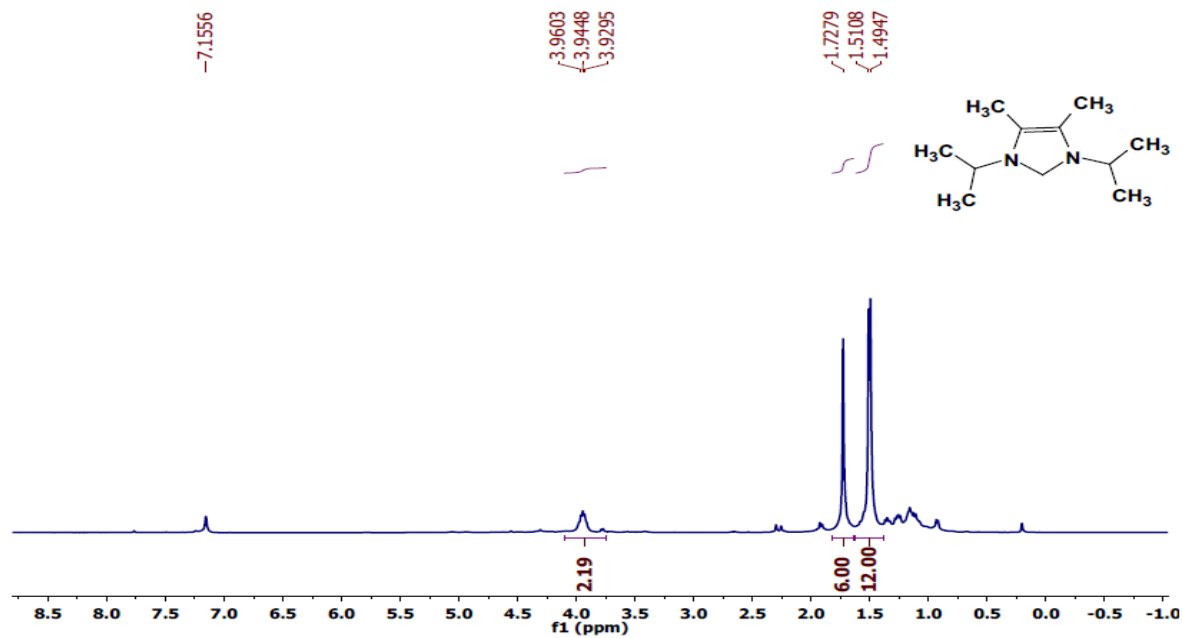


Figure 18: ^1H NMR Spectra of 1,3-diisopropyl-4,5-dimethylimidazol-2-ylidene after the experiment

3.1.2 FTIR Study:

We also recorded the IR spectra of 1,3-diisopropyl-4,5 dimethylimidazol-2-ylidene (NHC) in Nujol, which is shown in **Fig. 19**. After discounting the peaks due to the solvent Nujol, it can be seen that the major peaks for pure NHC lie between $2970\text{-}2873\text{cm}^{-1}$, which are essentially due to CH_3 stretches of methyl and isopropyl groups. The features at $1332, 1360\text{cm}^{-1}$ corresponds to anti symmetric and symmetric ring modes. The features at $1400\text{-}1600\text{cm}^{-1}$ are due to the bending mods of CH_3 groups. To confirm that these features do indeed correspond to the NHC, we have also presented the computed scaled spectra for the NHC for comparison, with the experimentally recorded spectra for NHC. It can be seen that there is a good agreement of the experimental spectrum with the computed spectrum, thereby confirming that the substrate is indeed NHC.

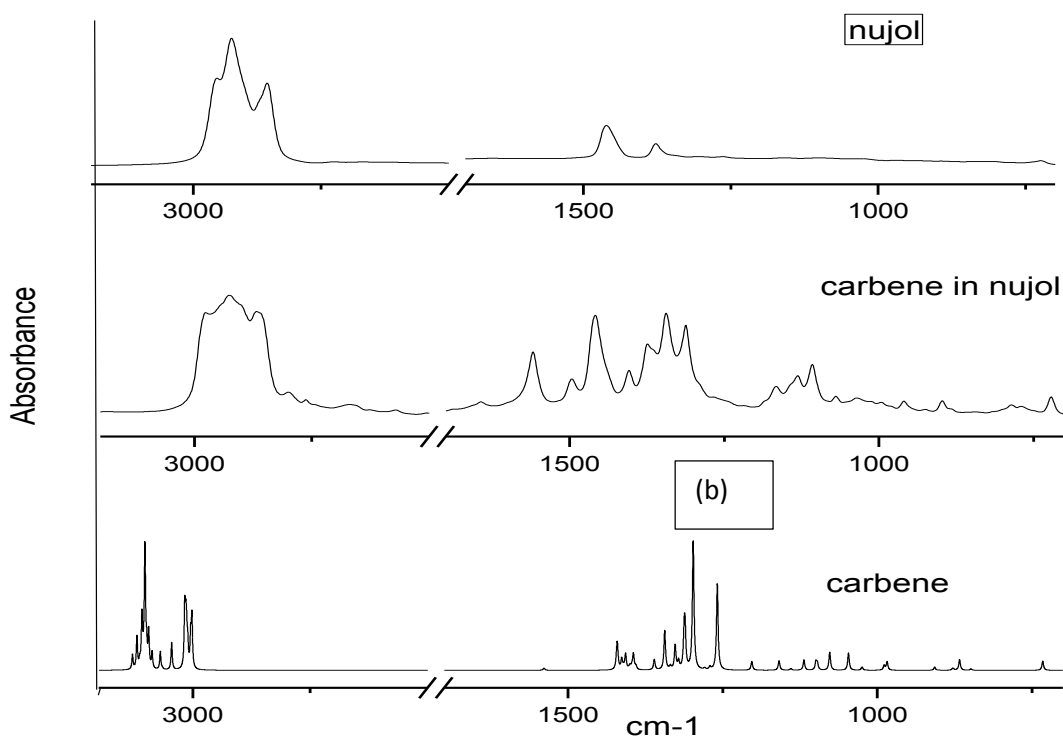


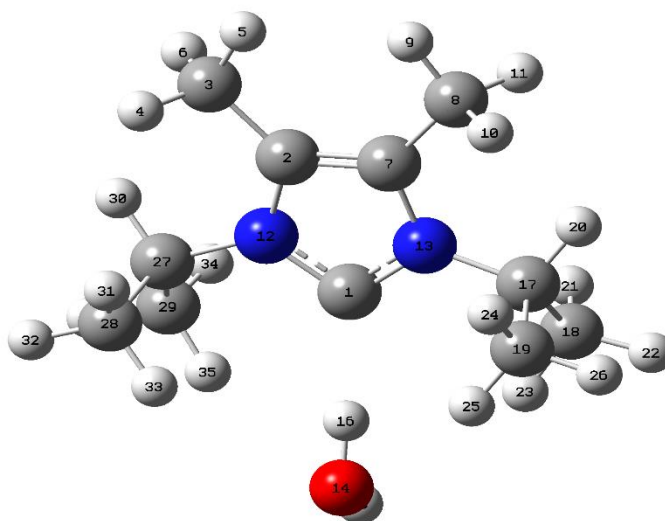
Figure 19: Spectra of Nujol, Carbene in Nujol and Computed spectra of carbene

Our ^1H and ^{13}C NMR and IR spectra therefore confirm the identity of the NHC substrate that we were using in our experiments.

3.2 Computational results

3.2.1 Conformational analysis:

In 1,3-diisopropyl-4,5-dimethylimidazol-2-ylidene there are two isopropyl group. This gives rise to many conformations due to the orientation of the isopropyl groups. We located three different conformer. We can define all three conformers in terms of dihedral angle. The table 2 for all three conformer is give below and it can be seen that the three conformers are isoergic. Hence we will restrict our discussion for the complexes using conformer 1.



Conformer	Dihedral angel (H ₂₀ -C ₁₇ -N ₁₃ -C ₁)	Dihedral angel (H ₃₀ -C ₂₇ -N ₁₂ -C ₁)	Energy difference (kal/mol)
Conformer-1	162.72	-162.72	0
Conformer-2	15.21	-166.09	0.003
Conformer-3	-13.56	12.71	0.006

Table 2: Relationship between dihedral angle of all conformer

The energies were calculated at M062x/6-311++G (d,p) level of theory for all three conformers of NHC. By looking the energy differences between all three conformers we conclude that conformer-1 is the most stable among them and it will be global minima. It is only this conformer that we consider when studying complex formation.

3.2.2 Calculation for possible complexes

The possible complexes which can be formed from 1,3-diisopropyl-4,5-dimethylimidazol-2-ylidene and water by using M062X/6-311++G(d,p) and MP2/6-311++G(d,p) level of theory are given below.

- 1) **Complex 1:** Hydrogen of water acts as proton donor to the carbene carbon in 1,3-diisopropyl-4,5-dimethylimidazol-2-ylidene
- 2) **Complex 2a:** In this structure one proton of water acts as proton donor to the carbene carbon atom, and other proton interact with backbone (double bond) of the NHC
- 3) **Complex 2b:** In this structure, the proton of water interacts with nitrogen atom of the carbene.
- 4) **Complex 3:** Oxygen of the water acts as proton acceptor to the hydrogen attached to doubly bonded carbon in 1,3-diisopropyl-4,5-dimethylimidazol-2-ylidene
- 5) **Complex 4:** Very weak complex in which water is between two methyl groups of isopropyl and oxygen of water acts as proton acceptor to hydrogens of two methyl groups.

The stabilization energies along with ZPE (zero point energy) and BSSE correction are tabulated. Among the all complexes, complex 1 is the most stable followed by complex 2a, complex 2b, complex 3, complex 4. Complex 2b and complex 4 did not optimized at MP2/6-311++G(d,p) level of theory.

Frequency calculations were performed at the same level of theory. For all complexes, all the frequencies were found to be positive, which shows that the all structure obtained are minima on the potential energy surfaces. In the complexes obtained at this level, the O-H and O-D stretching modes are red shifted as shown in **fig. 20**

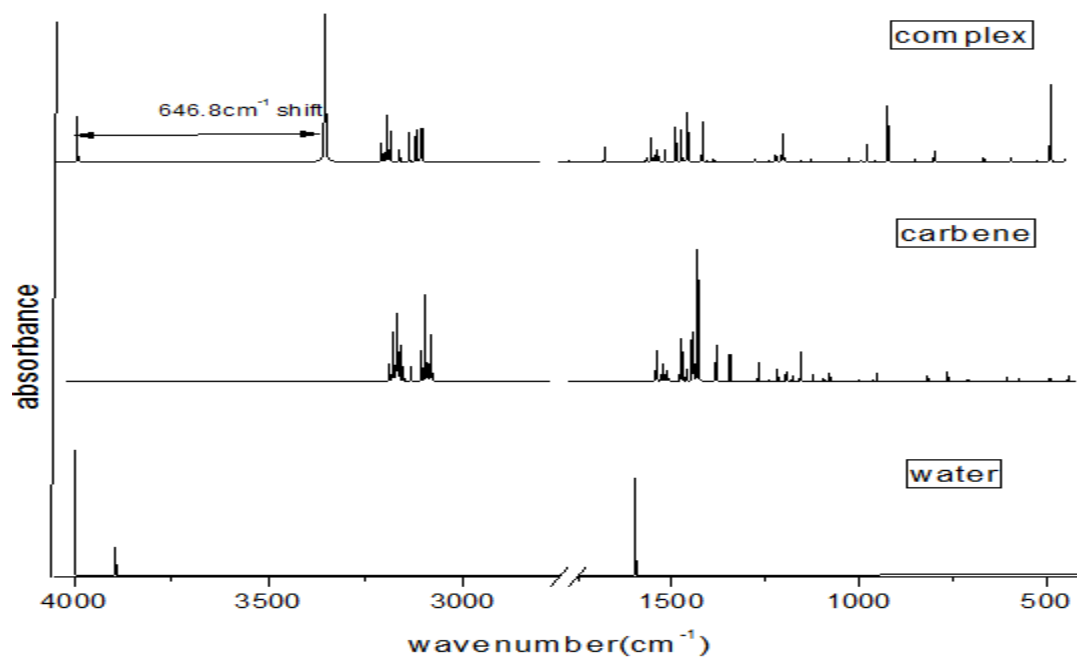
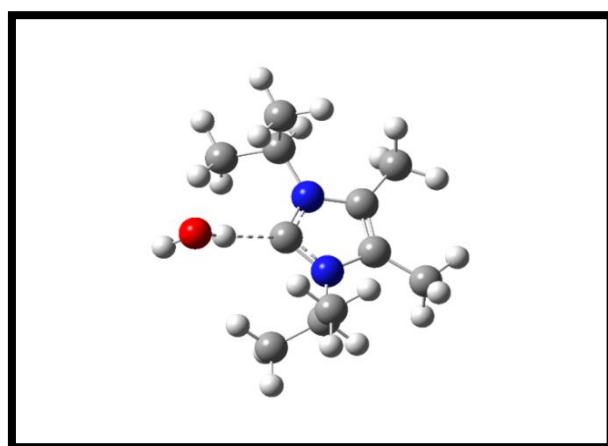
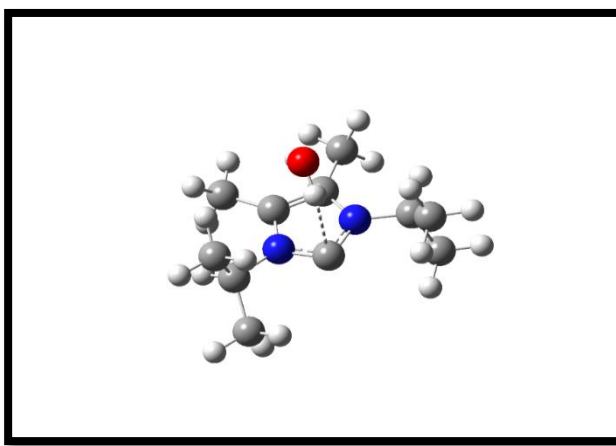


Figure 20: Computed IR spectra of carbene, water and complex at MP2/6-311++G(d,p) level of theory.

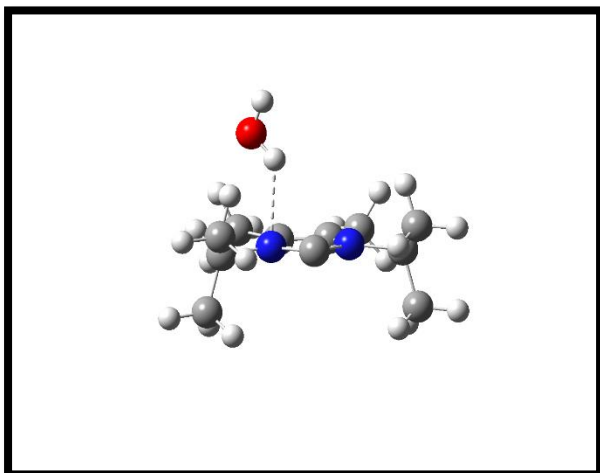
3.2.3 Optimized geometries obtained at M062X/6-311++G(d,p) and MP2/6-311++G(d,p) with their stabilization energies for complexes of NHC with Water given below:



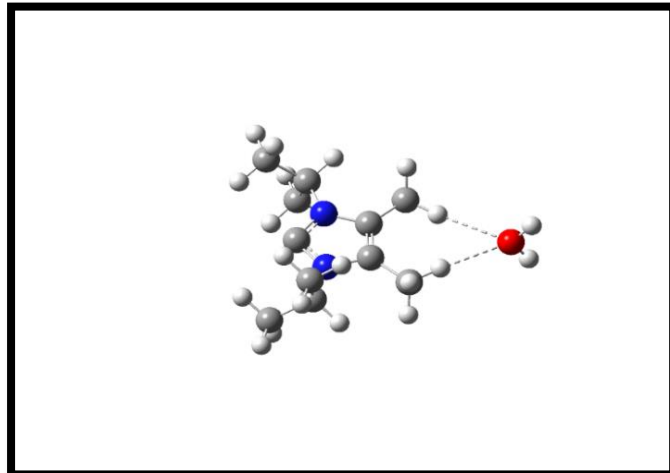
Complex-1



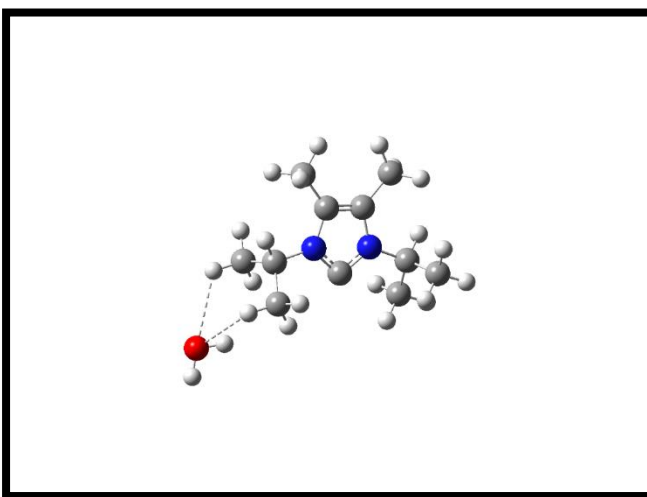
Complex-2a



Complex-2b



Complex3



Complex-4

Figure 21: Structures of optimized geometries obtained for the five different complexes

Table 3: Computed stabilization energy (in Kcal/mol) of NHC-H₂O complexes. Raw/ZPE/BSSE corrected energy values:

	Complex	M06-2x/6-311++G**	MP2/6-311++g**
1.	Complex-1	12.19/10.28/11.43	12.29/10.16/9.28
2.	Complex-2a	8.56/6.72/7.30	8.40/6.82/4.87
3.	Complex-2b	6.84/5.37/5.88	Not Optimized
4	Complex-3	3.08/1.91/1.73	3.40/2.07/1.62
5	Complex-4	2.65/1.57/0.75	Not Optimized

3.3 Experimental:

Matrix isolation experiments were performed in a N₂ matrix to study the NHC interaction with H₂O and D₂O. Experiments were performed at various conditions to optimize the deposition conditions. It was found that to obtain a good infrared spectrum, the NHC had to be maintained at ~7⁰. The temperature was maintained using a water-ice bath. The experiments were done using both single and double jet nozzles.

3.3.1 Matrix isolation infrared spectra of 1,3-diisopropyl-4,5-dimethylimidazol-2-ylidene(NHC)

Fig. 22 shows the infrared spectrum of NHC, in a nitrogen matrix. Typically about 3 mmoles of nitrogen was deposited on the KBr substrate along with the NHC. The deposition rate was about 3 mmoles/hr and a deposition lasted for about 45 minutes.

The main features in the spectrum are those due to the C-H stretches of the alkyl groups present in the NHC. The small feature seen at 3727 cm⁻¹ is due to water, which though not deliberately deposited, appears in all spectra as an ubiquitous impurity.

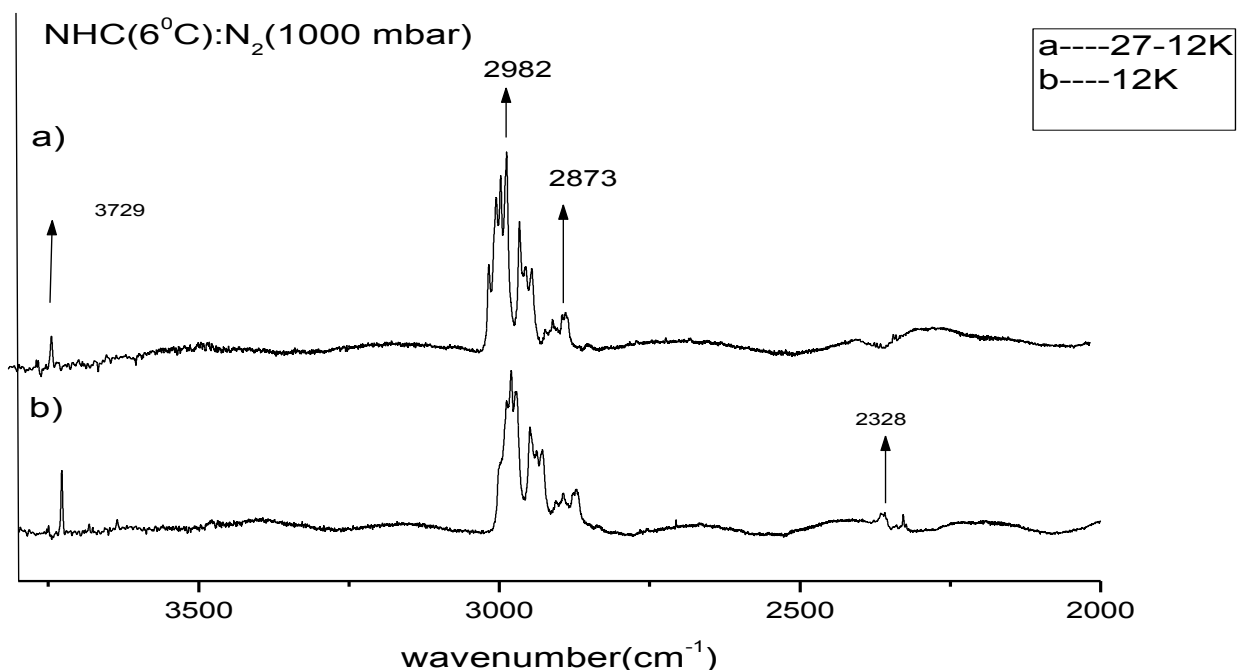


Figure 22: Spectral feature of 1, 3-diisopropyl-4-5-dimethylimidazol-2-ylidene in N₂ matrix (a) after annealing (b) before annealing

After deposition of NHC in N₂ matrix, and recording a spectrum at 12K, we annealed the matrix at 27 K for about an hour. This was a process to encourage the diffusion of the substrates and result in complex formation. As a result of complex formation, new features can be expected to be observed in the spectra.

3.3.2 Matrix isolation infrared spectra of H₂O and D₂O:

Experiments were now performed where the NHC and water were codeposited. The relative ratios of NHC and water were adjusted by altering the vapor pressures of each substrate by maintaining the appropriate temperatures. The anti-symmetric stretch of H₂O appears at 3727cm⁻¹, while the symmetric stretch occurs at 3635cm⁻¹. The bending mode can be observed at 1597cm⁻¹. Experiments were also conducted where NHC was codeposited with D₂O in N₂ matrix. The spectral feature for D₂O appears at 2765cm⁻¹, 2655cm⁻¹ and 1179cm⁻¹ for each of the modes referred to above.

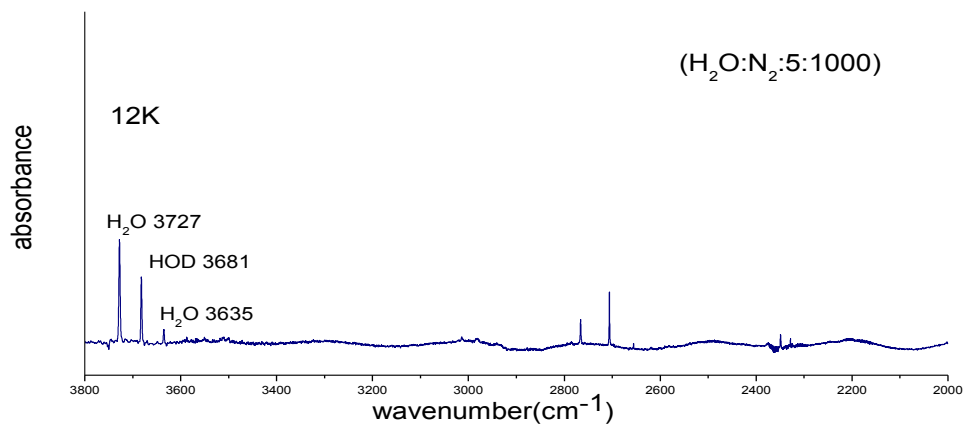


Figure 23: Experimental spectra of H₂O in N₂ Matrix in the ratio of (5:1000) at 12K

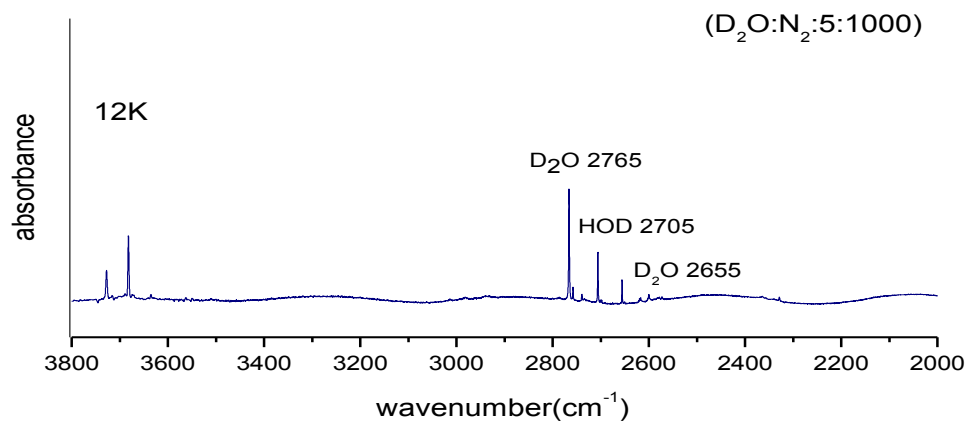


Figure 24: Experimental spectra of D₂O in N₂ matrix in the ratio of (5:1000) at 12K

3.3.3 Matrix isolation spectra of NHC-H₂O and NHC-D₂O complexes

In the codeposition experiments of NHC-H₂O, the features of H₂O in the complex was computed to occur near 2880 cm⁻¹. A careful examination of this region did reveal a feature near 2884.4 cm⁻¹ (Fig. 23). While it is certainly no conclusive, it is likely that this feature may be due to the NHC-water product. More experiments would necessarily have to be done to confirm the origin of this feature.

We therefore thought it might help if we performed codeposition experiments with D₂O, so that the red shifted feature of the NHC-D₂O can also be identified if they do appear in the spectra. The isotope shift would clearly confirm the assignment. Hence experiments were also performed with D₂O for the above purpose.

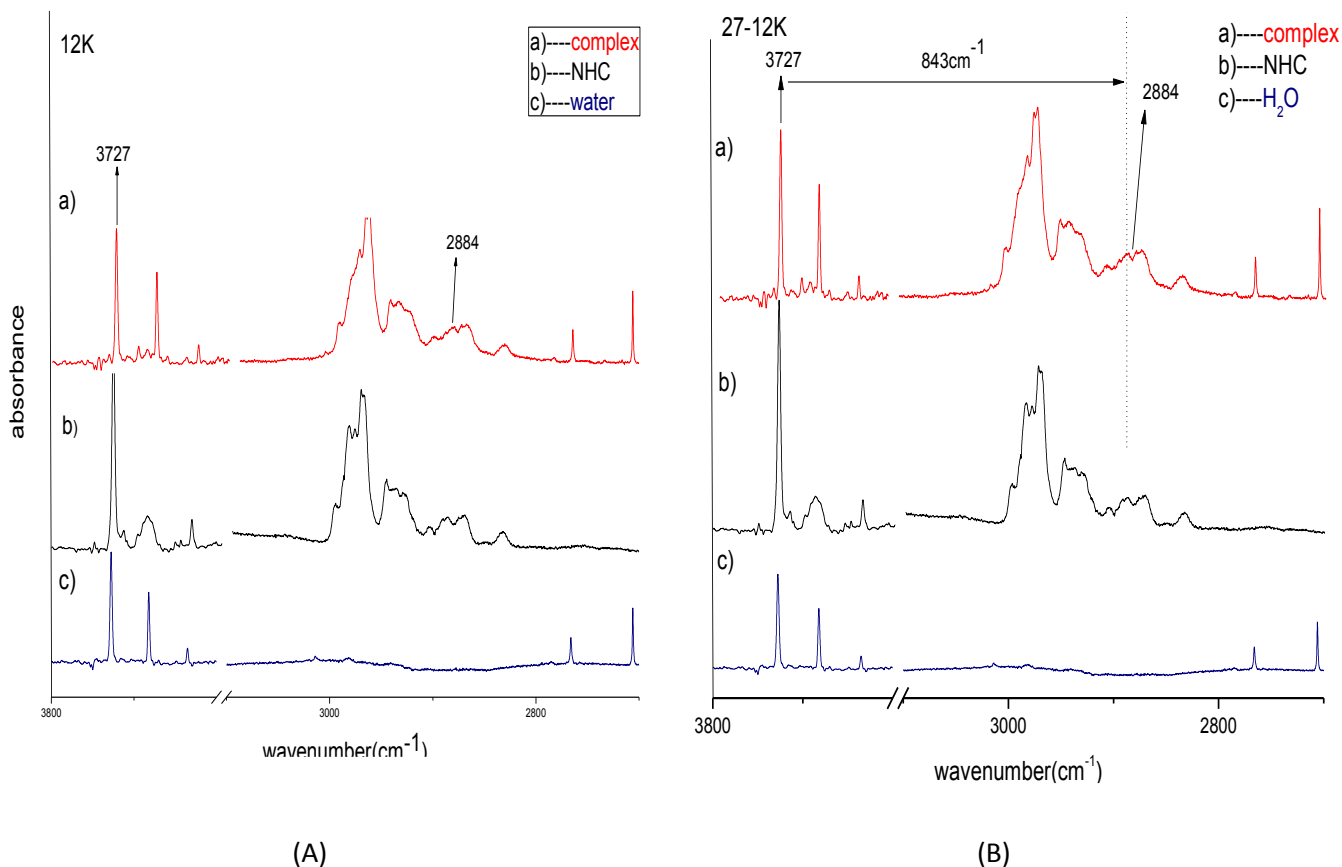


Figure 25: Comparison of IR spectra of complex, NHC and H₂O. (A) Before annealing (B) After the Annealing. (a) NHC (7⁰C): H₂O:N₂ (5:1000), (b) NHC (7⁰C):N₂ (1000) and (c) H₂O:N₂ (5:1000)

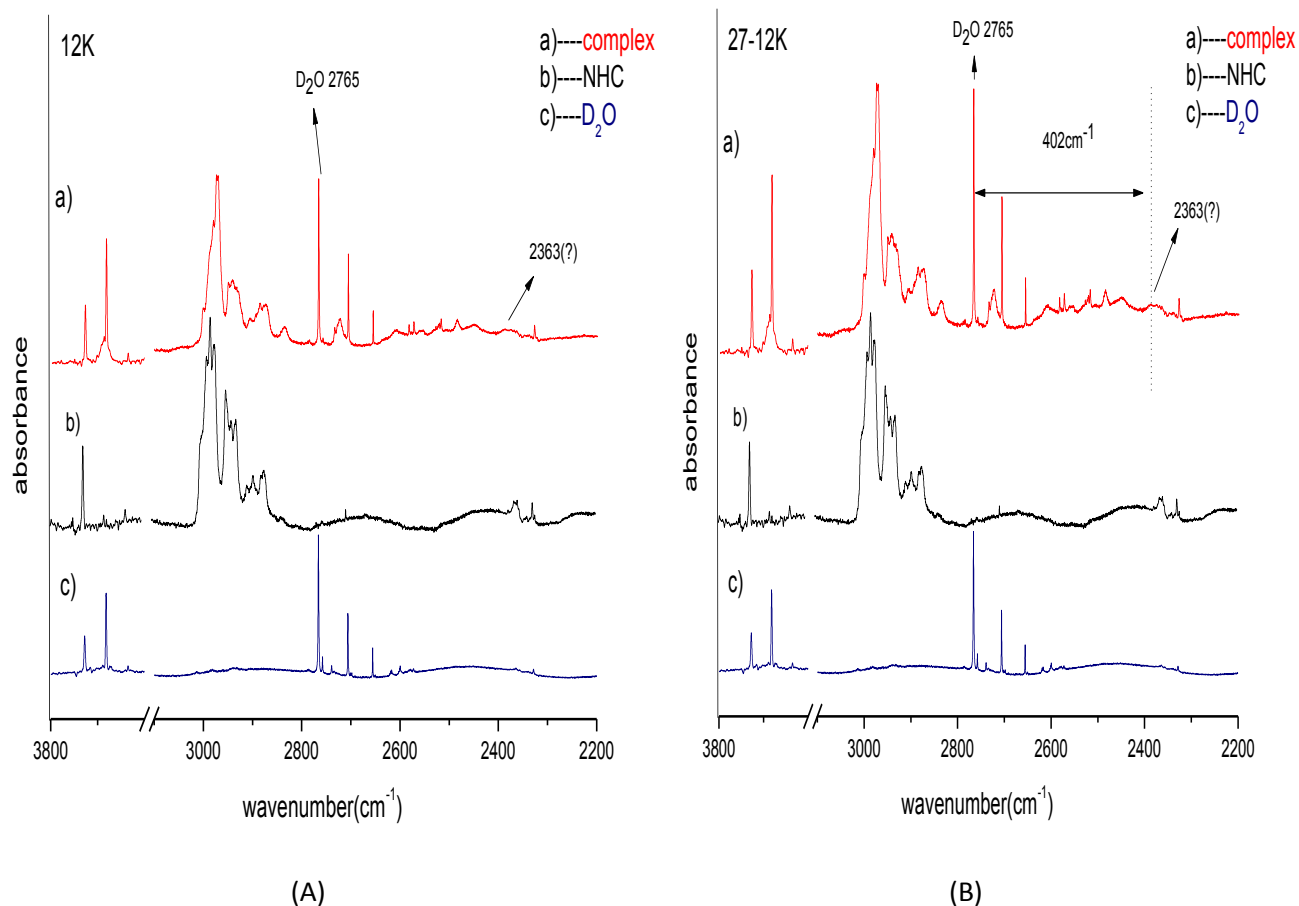


Figure 26: Comparison of IR spectra of complex, NHC and D₂O. (A) Before annealing (B) After the Annealing. (a) NHC (7⁰C):D₂O:N₂ (5:1000), (b) NHC (7⁰C):N₂ (1000) and (c) D₂O:N₂ (5:1000)

3.3.4 Experimental and vibrational analysis

The experimental spectra of 1,3-diisopropyl-4,5-dimethylimidazol-2-ylidene and its complex with H₂O and D₂O in N₂ matrix are shown in fig. 25 and 26 respectively. The figure shows spectra recorded both at 12K and that recorded after the matrix is annealed at 27 K. The feature due to the complex 1 is computed to occur at 2884.4cm⁻¹ for the OH stretch and at 2363 cm⁻¹ for the OD stretch. Since complex-1 is the most stable complex among all complexes, it is likely that complex 1 would be observed experimentally. In the nitrogen matrix, weak product features appear red shifted by 843.1 cm⁻¹ in the O-H stretch of water and 402.81 in the O-D stretch of D₂O. These features are in general agreement with the computed shifts of

646.8cm⁻¹ for the O-H modes. However, given that these features are extremely weak, more experiments are clearly required for confirming their origin.

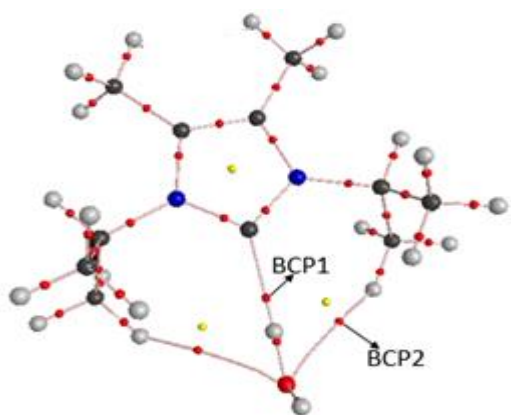
It must also be recognized that the hydrogen bonding in these complexes being so strong the normal mode picture of the H₂O vibrations break down. The vibrations of water can no longer be assigned as symmetric and anti-symmetric stretch, but as bound and unbound O-H.

3.4 AIM Analysis:

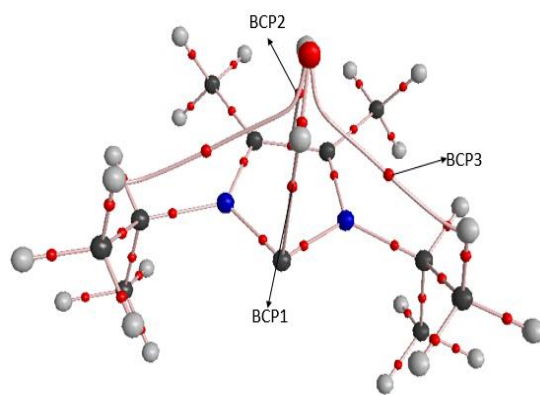
In this section we calculate electron charge density at bond critical point (BCP) and the Laplacian of charge density for different types of complexes as shown in Table 4. The electron density at the bond critical point (BCP1), is large with a value of 0.038 e/(bohr)³ between carbene carbon atom and hydrogen of water. This implies that the hydrogen bond interaction between NHC and H₂O in complex-1 is stronger than in any of the other complexes. In complex-1, water also have weak interaction with hydrogen of isopropyl groups and forms two seven member rings which may be makes it more stable than other complexes.

In complex-2a water interact with NHC in stacked fashion. This is second most stable complex was observed computationally. The electron density was found between carbene carbon and hydrogen of water at BCP1 is around 0.012 e/(bohr)³. In this structure water also interacts with hydrogen of two isopropyl groups and the double bond of the NHC.

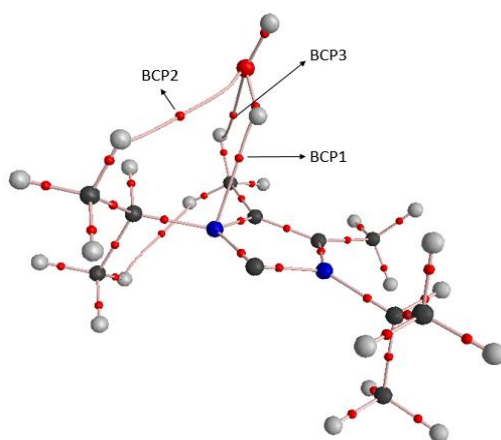
In complex-2b, which was the next in terms of the interaction energy, at the M062X/6-311++G(d,p) level of theory, the electron density was found around 0.012 e/(bohr)³ at BCP1. This structure could not be located at MP2/6-311++G(d,p) level of theory.



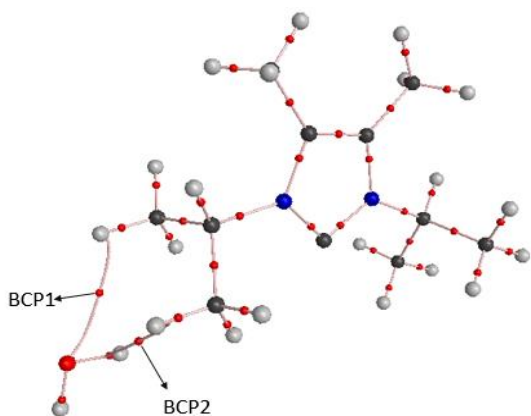
Complex-1



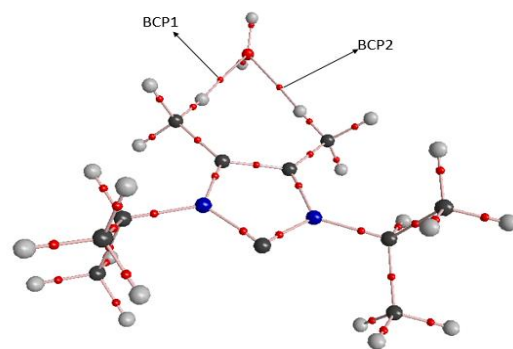
Complex-2a



Complex-2b



Complex-4



Complex-3

Figure 27: AIM structure of all complexes showing the bond critical points

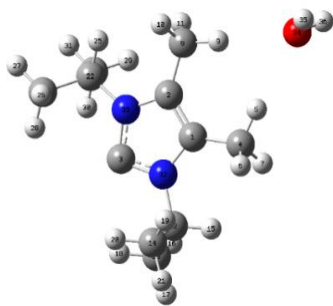
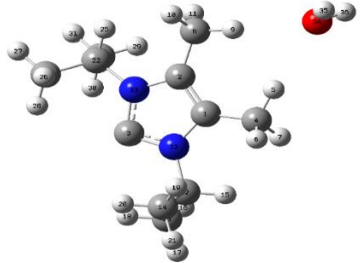
Table 4: Aim calculations for 1,3-diisopropyl-4,5-dimethylimidazol-2-ylidene and water complexes

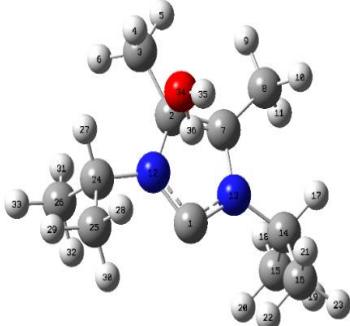
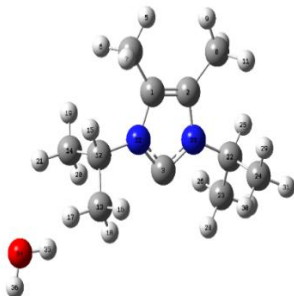
Complex	Critical point	$\rho(r_c)$	$\Delta^2\rho(r_c)$
Complex 1 MP2/6-311++G(d,p)	BCP1	0.0380929	0.0696
	BCP2	0.0057198	0.019486
Complex 2a MP2/6-311++G(d,p)	BCP1	0.01252	0.037231
	BCP2	0.00842	0.026431
	BCP3	0.00418	0.01538
Complex-2b M062x/6-311++G(d,p)	BCP1	0.01494	0.055357
	BCP2	0.00636	0.022042
	BCP3	0.00612	0.022247
Complex-3 MP2/6-311++G(d,p)	BCP1	0.00865	0.029121
	BCP2	0.00868	0.028962
Complex-4 M062x/6-311++G(d,p)	BCP1	0.00702	0.028595
	BCP2	0.00734	0.027178

Table 5: Some selected geometrical parameters of complexes at M062X/6-311++G(d,p) and MP2/6-311++G(d,p), where bond length is given in Å, bond angle in degree :

Complex-1	M062x/6-311++g(d,p)	MP2/6-311++g(d,p)
r(C1-H16)	1.92	1.92
r(O14-H16)	0.98	0.99
r(O14-H15)	0.96	0.96
r(C1-N12)	1.35	1.37
r(C2-C7)	1.36	1.38
N12-C1-H16	126.34	125.08
C1-H16-O14	172.25	170.90
N13-C1-N12	103.18	102.32
H15-O14-H16-C1	179.99	179.98

Complex2a	M062x/6-311++g(d,p)	MP2/6-311++g(d,p)
C3-H36	2.46	2.40
H29-O34	2.83	3.00
H16-O34	2.94	3.01
H35-C1	2.60	2.69
N32-C3-N33	102.37	101.57
O34-H36-C3	128.70	135.55
H35-O34-H36-C3	3.22	1.06

Complex-3	M062x/6-311++g(d,p)	MP2/6-311++g(d,p)
		
O34-H5	2.43	2.47
O34-H9	2.43	2.47
N33-C3-N32	102.21	101.47
H36-O34-H5	121.07	123.01
H35-O34-H9-C8	4.27	29.66

Complex2b	M062x/6-311++g(d,p)	Complex-4	M062x/6-311++g(d,p)
			
N12-H36	2.25	O34-H21	2.59
H36-C1	2.62	O34-H17	2.73
O34-H28	2.77		
O34-H4	2.70		
N12-C1-N13	102.19		
O34-H36-C1	160.66		
H35-O34-H36-C1	165.91		

3.5 Discussion

In the N₂ matrix, the feature due to the complex were observed at 2884cm⁻¹ for the O-H stretch and 2363cm⁻¹ for the O-D stretch were observed. In the water monomer, the normal modes are designated as anti-symmetric and symmetric stretches. However, in the hydrogen bonded NHC-H₂O complexes, the strong interaction, breaks down the normal mode picture and the vibrations of water have to be designated as bound and unbound O-H and O-D stretches. The large red shift of 843cm⁻¹ found for complex 1 in the N₂ matrix, indicates a strong hydrogen bond in operation in this complex.

N ₂ Matrix	Calculated frequencies	Scaled frequencies	Scaling factor	Experimental frequencies(cm ⁻¹)	Computed shift(cm ⁻¹)	Experimental shift(cm ⁻¹)	Mode of assignment
D ₂ O	2933.6		0.9427	2765.8			Asym. OD stretch
Water	4005.5		0.9305	3727.3			Asym. OH stretch
Complex1 (OH bound)	3310.3	3080.4	0.9305	2884.4	-646.8	-843.1	Bound OH to carbene
Complex 1(OD bound)	2409.1	2271.3	0.9427	2363.2	-494.5	-402.8	Bound OD to carbene

$$\text{Frequency Shift } (\Delta\nu) = (\text{Monomer Frequency}) - (\text{Complex Frequency})$$

Chapter-4

Conclusions

The thesis provides computational and experimental study of strong hydrogen bond interaction between N-heterocyclic carbene and water. The experiments study is done by matrix isolation infrared spectroscopy. The NHC was identify by ^{13}C and ^1H NMR spectroscopy. The feature at 207 ppm in the ^{13}C NMR confirmed the product to be the carbene. The computational study is done by Gaussian09 programme and the computational analysis has performed at M062x and MP2 method using 6-311++G(d,p) basis set. There were five complexes observed computationally. The stability order of all complexes: complex-1 > complex-2a > complex-2b > complex-3 > complex-4. The stabilization energy of complex 1 found to be 9.2kcal/mol which indicate the strong hydrogen bond interaction between NHC and H_2O . In experimental very weak feature at 2884.4cm^{-1} for water complex with the red shift of 843.1cm^{-1} is could be the product peak. These features are in good agreement with the computed shifts of 646.8cm^{-1} for the O-H modes. However, given that these features are extremely weak, more experiments are clearly required for confirming their origin.

Bibliography

- ⁱ Feller, D.; Borden, W. T.; Davidson, E. R. *Chem. Phys. Lett.* **1980**, 71, 22.
- ⁱⁱ Bauschlicher, C. W., Jr.; Schaefer, H. F., III; Bagus, P. S. *J. Am. Chem. Soc.* **1997**, 99, 7106.
- ⁱⁱⁱ Schuster, G. B. *Adv. Phys. Org. Chem.* **1986**, 22, 311
- ^{iv} Carter, E. A.; Goddard III, W. A. *J. Chem. Soc.* **1987**, 86, 862, there references.
- ^v Bourissou, D.; Guerret, O.; Gabbai, F. P.; Bertrand, G. *Chem. Rev.* **2000**, 100.39-91
- ^{vi} Osborn, D. L.; Vogelhuber, K. M.; Wren, S. W.; Miller, E. M.; Yu-Ju Lu; Case, A. S.; Sheps, L.; McMahon, R. J.; Stanton, J. F.; Harding, L. B.; Ruscic, B.; Lineberger, W. C.; *J. Am. Chem. Soc.* **2014**, 136, 10361–10372
- ^{vii} *J. Am. Chem. Soc.* **2001**, 123, 7188-7189, *J. Am. Chem. Soc.* **2005**, 127, 7294-7295, *J. Am. Chem. Soc.* **2004**, 126, 10212-10213
- ^{viii} Wanzlick, H. W. ; Schonherr, H.J. *Angew. Chem.* **1968**, 80,154.
- ^{ix} Arduengo, A. J.; Harlow, R. L.; Kline, M. *J. Am. Chem. Soc.* **1991**, 113, 361
- ^x Sander, W.; Bucher, G.; Wierlacher, S., *Chem. Rev.*, **1993**, 93 (4), pp 1583–1621
- ^{xi} Nakamoto, Kazuo; Margoshes, Marvin; Rundle, R.E., *J. Am. Chem. Soc.* **1955**, 77, 6480-6486
- ^{xii} Duarte, L.; Khriachtchev, L.; *RSC Adv.*, **2017**,7, 813-820
- ^{xiii} Mielke, Z.; Coussan, S.; Mierzwicki, K.; Roubin, P.; Sałdyka, M. *J Phys Chem A.* **2006**, Apr 13; 110(14):4712-8.
- ^{xiv} K. Morokuma and L. Pedersen, *J. Chem. Phys.* **1968**, 48, 3275
- ^{xv} Raut, A. H.; Karir, G.; Viswanathan, K. S.; *J. Phys. Chem. A*, **2016**, 120 (47), pp 9390–9400
- ^{xvi} Costa, P.; Sander, w.; *Angew, Chem, Int. Ed.* **2014**,53, 5122-5125
- ^{xvii} E. Whittle, D. A. Dows, G. C. Pimentel, *J. Chem. Phys.* **1954**, 22, 1943
- ^{xviii} Hallam, H. E. *Vibrational Spectroscopy of trapped Species* (Wiely Inter science publication, London, 1973)
- ^{xix} Pimentel, G. C; Charles, S. W. *Pure and Appl. Chem.* **1963**, 7, 111

^{xx} Matrix Isolation: A Technique for the Study of Reactive Inorganic Species, by Stephen Cradock

^{xxi} Owen Byrne, PhD Thesis, NUI Maynooth Press, **2009**.

^{xxii} <http://www.ccl.net/cca/documents/dyoung/topics-orig/compchem.html>

^{xxiii} Gaussian 09, Revision A.02, M. J. Frisch, G. W. Trucks, H. B. Schlegel, G. E. Scuseria, M. A. Robb, J. R. Cheeseman, G. Scalmani, V. Barone, G. A. Petersson, H. Nakatsuji, X. Li, M. Caricato, A. Marenich, J. Bloino, B. G. Janesko, R. Gomperts, B. Mennucci, H. P. Hratchian, J. V. Ortiz, A. F. Izmaylov, J. L. Sonnenberg, D. Williams-Young, F. Ding, F. Lipparini, F. Egidi, J. Goings, B. Peng, A. Petrone, T. Henderson, D. Ranasinghe, V. G. Zakrzewski, J. Gao, N. Rega, G. Zheng, W. Liang, M. Hada, M. Ehara, K. Toyota, R. Fukuda, J. Hasegawa, M. Ishida, T. Nakajima, Y. Honda, O. Kitao, H. Nakai, T. Vreven, K. Throssell, J. A. Montgomery, Jr., J. E. Peralta, F. Ogliaro, M. Bearpark, J. J. Heyd, E. Brothers, K. N. Kudin, V. N. Staroverov, T. Keith, R. Kobayashi, J. Normand, K. Raghavachari, A. Rendell, J. C. Burant, S. S. Iyengar, J. Tomasi, M. Cossi, J. M. Millam, M. Klene, C. Adamo, R. Cammi, J. W. Ochterski, R. L. Martin, K. Morokuma, O. Farkas, J. B. Foresman, and D. J. Fox, Gaussian, Inc., Wallingford CT, 2016.

^{xxiv} Lewars, E. Computational Chemistry: Introduction to the theory and applications of molecular and quantum mechanics. Kluwer Academic publishers, 2003

^{xxvi} ATOM IN MOLECULES A QUATUM THEORY BY RICHARD F. W. BADER